Schweizerische Eidgenossenschaft
Confédération suisse
Confederazione Svizzera
Confederaziun svizra

Federal Department of the Environment, Transport, Energy and Communications DETEC

Swiss Federal Office of Energy SFOE
Energy Research and Cleantech

Final report

RACONT2050

Reliability and Comparison of New PV-Technologies in Systems

University of Applied Sciences and Arts
of Southern Switzerland

SUPSI

Date: 23.12.2025

Location: Bern

Publisher:
Swiss Federal Office of Energy SFOE
Energy Research and Cleantech
CH-3003 Bern
www.bfe.admin.ch

Subsidy recipients:
Scuola universitaria professionale della Svizzera italiana (SUPSI)
Campus Mendrisio, Via Flora Ruchat-Roncati 15, CH-6850 Mendrisio
www.supsi.ch

Authors:
Domenico Chianese, SUPSI, domenico.chianese@supsi.ch
Gabi Friesen, SUPSI, gabi.friesen@supsi.ch
Bert Herteleer, SUPSI, bert.herteleer@supsi.ch
Mauro Caccivio, SUPSI, mauro.caccivio@supsi.ch

SFOE project coordinator:
Stefan Oberholzer, Swiss Federal Office of Energy, stefan.oberholzer@bfe.admin.ch

SFOE contract number: SI/502264-01

Acknowledgements

The authors of this report would like to thank all colleagues of ISAAC without whom all this work would not have been possible, and particularly:

- **Nicolas Ostinelli, Enrico Burà, Boris Margna and Pasquale Granato** (ISAAC/ENG team) for the development and maintenance of Campus Viganello PV systems, for the installation of Campus Trevano PV system and monitoring and for all the IT infrastructure.

- **Giovanni Bellenda, Flavio Valoti, Mattia Ceretti and Moreno Ronchi** (ISAAC/PVLab team) for all indoor measurements and management of reference modules.

- **Tyler Bacciarini**
for the development of the InfluxDB exporter.

- **Samuele Chiesa,** master student and **Gian Carlo Dozio,** master Thesis Responsible, SUPSI-DTI
for the development of the Dark I-V string monitoring (1500 V, 20A).

- **Roberto Mallone,** Elettroconsulenze SA
for the coordination of electricians, the project and purchasing.

- **Alfredo Michea**, Project Manager at Bouygues E&S InTec Svizzera SA
for the construction of the PV system at the Viganello Campus

- **Roberto Ricciardi**, Project Manager Monitoring at Siemens Schweiz AG
for the development of the monitoring system integrated into the building management system.

and all the colleagues and SUPSI staff who collaborated in one way or another to the realization of the project.

Summary

The RACONT2050 project investigates the performance and reliability of main-stream crystalline silicon photovoltaic (PV) technologies under real operating conditions. Rapid innovation in PV modules, such as new cell architectures (PERC, TOPCon, HJT) and the use of new materials, has led to higher efficiencies but also introduced new and not yet fully understood risks related to long-term reliability. Building on the legacy of the historic TISO-10 installation, the project establishes a large-scale experimental platform in Switzerland to systematically compare these technologies and generate long-term data up to 2050.

To address these challenges, a 132 kWp PV system was installed on two rooftops of the USI/SUPSI campus in Viganello, deploying seven state-of-the-art module technologies from five manufacturers across ten independently monitored high-voltage (up to 1500 V) strings. A complementary low-voltage reference system was built in Trevano alongside the original 1982 TISO installation, enabling both technological and historical comparisons. The project combines detailed laboratory testing with continuous field monitoring and develops advanced diagnostic tools, most notably a novel dark I–V measurement system capable of detecting faults and degradation mechanisms at string level. This integrated approach enables the demonstration of modern PV technologies, the evaluation of early-stage reliability, the assessment of system-level effects (e.g. voltage and shading), and the establishment of a long-term monitoring platform.

The results show that most technologies perform reliably in their early operational phase, with degradation rates generally within manufacturers' warranty limits. However, clear differences between technologies were observed. TOPCon modules demonstrated the best overall performance, achieving higher energy yields than both PERC and HJT technologies. In contrast, HJT modules showed significantly higher early degradation and some material-related issues, highlighting the importance of independent testing before large-scale deployment. Additional findings include a systematic overestimation of module power ratings by manufacturers, occasional mechanical failures such as glass breakage, and operational challenges related to high-voltage system components. Overall system performance was high, with strong performance ratios across all technologies.

Take-Home Messages

1. **TOPCon technology currently delivers the best overall performance, confirming the ongoing technological shift in photovoltaics,** providing a robust basis for investment and support decisions within Switzerland's Energy strategy 2050.
2. **Some module technologies show higher early degradation and reliability risks - linked to issues such as glass breakage and cell interconnection failures -** highlighting the importance of independent testing and early field testing to reduce risks in the large-scale expansion of PV capacity in Switzerland.
3. **A novel string-level dark I–V diagnostic tool was developed and validated for high-voltage (1500 V) PV systems,** demonstrating strong potential for early fault detection and improved system reliability, with future implementation planned in follow-up projects.
4. **The RACONT2050PV demonstration system provides a high-resolution reference installation and dataset for long-term comparison, degradation analysis, benchmarking, and follow-up projects,** supporting innovation, system design, quality assurance, and evidence-based decision-making in Switzerland's energy transition.

Zusammenfassung

Das Projekt RACONT2050 untersucht die Leistungsfähigkeit und Zuverlässigkeit marktüblicher kristalliner Silizium-Photovoltaik-(PV)-Technologien unter realen Betriebsbedingungen. Die rasche Innovation bei PV-Modulen, wie neue Zellarchitekturen (PERC, TOPCon, HJT) und der Einsatz neuer Materialien, hat zu höheren Wirkungsgraden geführt, gleichzeitig aber auch neue und bislang nicht vollständig verstandene Risiken hinsichtlich der Langzeitzuverlässigkeit eingeführt. Aufbauend auf dem Erbe der historischen TISO-10-Anlage etabliert das Projekt eine repräsentative experimentelle Plattform in der Schweiz, um diese Technologien systematisch zu vergleichen und Langzeitdaten bis 2050 zu generieren.

Zur Adressierung dieser Herausforderungen wurde eine 132 kWp PV-Anlage auf zwei Dächern des USI/SUPSI-Campus in Viganello installiert. Dabei kommen sieben moderne Modultechnologien von fünf Herstellern in zehn unabhängig überwachten Hochvolt-Strings (bis zu 1500 V) zum Einsatz. Ein ergänzendes Niedervolt-Referenzsystem wurde in Trevano neben der ursprünglichen TISO-Anlage von 1982 aufgebaut, wodurch sowohl technologische als auch historische Vergleiche ermöglicht werden. Das Projekt kombiniert detaillierte Labortests mit kontinuierlichem Feldmonitoring und entwickelt fortschrittliche Diagnosewerkzeuge, insbesondere ein innovatives Dark-I–V-Messsystem, das Fehler und Degradationsmechanismen auf String-Ebene erkennen kann. Dieser integrierte Ansatz ermöglicht die Demonstration moderner PV-Technologien, die Bewertung der Frühzuverlässigkeit, die Analyse von Systemeffekten (z. B. Spannung und Verschattung) sowie den Aufbau einer langfristigen Monitoring-Plattform.

Die Ergebnisse zeigen, dass die meisten Technologien in der frühen Betriebsphase zuverlässig funktionieren, wobei die Degradationsraten im Allgemeinen innerhalb der Herstellergarantie liegen. Dennoch wurden klare Unterschiede zwischen den Technologien festgestellt. TOPCon-Module zeigten die beste Gesamtleistung und erzielten höhere Energieerträge als sowohl PERC- als auch HJT-Technologien. Im Gegensatz dazu wiesen HJT-Module eine deutlich höhere Frühdegradation sowie materialbedingte Probleme auf, was die Bedeutung unabhängiger Tests vor einer grossflächigen Einführung unterstreicht. Weitere Ergebnisse umfassen eine systematische Überschätzung der Modulleistung durch Hersteller, vereinzelte mechanische Ausfälle wie Glasbruch sowie betriebliche Herausforderungen im Zusammenhang mit 1500 V Komponenten. Insgesamt zeigte das System eine hohe Leistungsfähigkeit mit starken Performance Ratios über alle Technologien hinweg.

Contents

Abbreviations

Bifi	Bifacial
EL	Electroluminescence
GCO	Electrical performance at various irradiances
G	Irradiance
Gpoa	Plane of array irradiance
η_N	Normalised efficiency
HC	Half-cut (cell)
Hpoa	Plane of array insolation
HJT	Heterojunction cell technology
IBC	Integrated back contact
IEC	International Electrotechnical Commission
Isc	Short-circuit current
I-V	Current-Voltage
kJ	kilo Joule
LID	Light Induced Degradation
ms	milli second
MBB	Multi Bus Bar
MPP(T)	Maximum Power Point (Tracker)
PAE	Prescrizioni Aziende Elettriche
PERC	Passivated Emitter and Rear Cell
PID	Potential induced degradation
Pm	Maximum Power under standard test conditions
Pnom	Nominal Power under standard test conditions (data sheet)
PR, PRtc	Performance ratio, temperature-corrected performance ratio
PV	Photovoltaics
SR	Spectral Response
STC	Standard Test Conditions
T	Temperature
Tbom	Back Of the Module Temperature
TCO	Temperature coefficients
Tmod	Module operating temperature
TOPCon	Tunnel Oxide Passivated Contact
TS	Technical standard
UTC	Coordinated Universal Time
UV	Ultraviolet
VI	Visual inspection
Voc	Open-circuit voltage
WL	Wet-leakage

1 Introduction

In recent years, numerous technological changes at both cell and module level were introduced into the photovoltaic (PV) market, with very fast mainstream uptake [1]. New high-efficiency cell designs such as **Passivated Emitter and Rear Cell (PERC), Tunnel Oxide Passivated Contact (TOPCon), and Heterojunction (HJT)** have been deployed. These technologies are typically based on larger wafers that are subsequently cut into half, thirds, or quarters and interconnected using advanced approaches such as Multi Bus Bar (MBB) or shingling connections. At the same time, solar cells rapidly evolved from monofacial to bifacial designs. Each cell technology has its own degradation and failure mode [2], and when combined with novel materials (encapsulants, backsheets) and processes (how cells are cut, soldering temperatures used, how these are then joined in modules) by manufacturers, can result in potential risks which affect long-term reliability.

The degradation modes of these novel cell and module designs differ significantly from those observed in the previous benchmark technology, which had stable performance, aluminium back surface field (Al-BSF). The relative importance of degradation mechanisms such as potential-induced degradation (PID), light-induced degradation (LID), light-and high-temperature induced degradation (LeTID), as well as UV-induced degradation (UVID) [3] varies across PERC, TOPCon, HJT. A further under-appreciated risk is the difference in performance and degradation behaviour between manufacturers producing the same nominal technology (e.g. TOPCon or HJT). Nevertheless, the cost-driven PV market often treats the modules as interchangeable commodities which can be easily replaced [1]. The following table lists some examples of the potential risk factors correlated to the introduction of technological innovations and their advantages.

Table 1: *Technological innovation advantages and potential risks.*

Innovation	Advantages	Potential risk factors
Half-cut cells	- lower ohmic losses - higher crack resistance - higher shading tolerance	- twice as many soldering connections where hot-spots can occur - cutting increases the risk of cell-inherent defects - shift of diode activation
Cell shingling/ tiling ribbons	- reduction of passive module area → higher power density - almost no ribbons → reduced costs and ribbon shading - no visible busbars - lower ohmic losses - lower processing temperatures - lower operating temperature	- durability of conductive glues - mechanical stresses - stresses due to different thermal expansion coefficients - misalignment of the cells - individual cells need to be made as uniform as possible to ensure tight connections between cells
Large area cells	- higher power density	- hot cells und partial shading→ material degradation - high currents → higher current-induced losses
High power/large area modules (>500W)/ thinner glass	- reduced costs - longer strings possible - reduced weight	- high string voltages in combination with transformer less inverters - mechanical stability and robustness - voltage induced degradation mechanism (e.g, PID)
Bifacial cells/modules	- capture of back side irradiance - higher power density	- increased current mismatch/hot-spots - major diode activation - lower mechanical strength with thinner glass - durability of transparent rear cover
Multi-wire/busbar cells	- lower ohmic losses - lower microcrack losses - lower impact of hot-spots	- more soldering connections - cold soldering - desoldering risks - manufacturing induced micro-crack caused by wire

The **RACONT2050** project addresses these challenges by investigating the performance and reliability of several new PV module technologies under real operating conditions in Switzerland. The project is inspired by the **Ticino Solare 10 kWp (TISO-10)** demonstration system, built by SUPSI in the early 1980s, using cutting-edge silicon PV modules available at the time. That system continues to operate and has generated numerous technical reports [4], [5], conference papers [6], [7] and journal articles [8], [9], [10], [11]. Building on the lessons learned from TISO-10, RACONT2050 aims to extend this concept by providing long-term insights for researchers, installers, and policymakers, while ensuring the continuity of monitoring data from the installed systems up to 2050.

The project investigates potential early-stage failures of new PV technologies that may arise under different system configurations through in-depth performance analysis combining laboratory measurements and field monitoring data. One important system variable investigated in RACONT2050 is the impact of string voltage. Module performance is evaluated under high string voltages of up to 1500 Vdc and compared with low-voltage strings (350 Vdc or less). This comparison provides insights into the risk of potential-induced degradation (PID) for these new module technologies, as PID has been shown to cause rapid and significant power losses in susceptible modules [12], [13].

To enable this investigation, a new commercial-scale high-voltage string demonstration system was built on the roofs of the USI/SUPSI campus at Viganello. The PV plant was completed in the winter of 2022 and put into operation in June 2023 due to legal issues between the stakeholders involved. The **Viganello system** has a nominal power of **132.12 kWp** distributed over two green roofs, with cutting-edge modules from five manufacturers, showcasing seven technologies, four monofacial and three bifacial module technologies. In 2023, the **Trevano system**, a second smaller installation with a capacity of **16.74 kWp** and configured with low-voltage strings was built with the remaining modules. This installation enables a direct comparison between old Al-BSF technology of 40 years ago and new technologies and, at the same time, to have a comparison of high-voltage to low-voltage strings.

To collect valuable long-term data, the project combines outdoor monitoring with detailed indoor laboratory characterisation of reference modules. Selected modules are therefore periodically removed from the installation and measured in the laboratory to quantify degradation and correlate laboratory measurements with field performance data. While laboratory and module-level measurements provide high-precision characterisation of individual modules, system-level monitoring allows the behaviour of a larger number of modules to be evaluated under realistic operating conditions. This approach captures the influence of electrical interactions within strings, system design constraints, and environmental factors such as soiling or albedo. High-resolution monitoring of irradiance, temperature, albedo, and soiling conditions further supports the interpretation of system behaviour.

A key innovation of RACONT2050 is the development of an automated Dark I-V Measurement System (DIVMS) capable of measuring full current-voltage characteristics of PV strings during nighttime operation. The system was specifically designed to operate at string voltages up to 1500 V and currents up to 20 A, exceeding the capabilities of currently available commercial instruments developed only for punctual field inspections. By enabling continuous dark I-V measurements, the system allows early or real-time detection of electrical faults and degradation mechanisms such as increased series resistance, shunt defects, bypass diode failures, and string-level mismatch effects.

The RACONT2050 installation will set the base for (1) the demonstration of long-term reliability beyond 2050 (over 30 years of lifetime) of selected state-of-the-art PV technologies in 2022 and (2) the collection of long-term data needed for the initiation of follow-up R&D projects on module reliability and lifetime prediction. When combined and compared with comparable systems monitored by other research institutions and companies, a more comprehensive view of the risks and benefits of these novel technologies will be obtained.

2 Project objectives

The RACONT2050 project aim is to investigate the performance and reliability of modern PV module technologies operating in real PV systems under Swiss climate conditions while also establishing a monitoring infrastructure that sets the basis for long-term performance and reliability studies extending towards 2050.

This project has both short-term (during the project) and long-term (up to 2050) objectives which are:

1. **Demonstration of modern PV technologies in real operating conditions**
   Deploy and operate a selected number of state-of-the-art PV module technologies within the same installation to enable direct comparison of their performance under (1) real system conditions and (2) identical environmental conditions.
2. **Evaluation of early-stage reliability of new PV technologies**
   Identify potential early degradation mechanisms and reliability issues associated with recent technological developments at cell and module levels.
3. **Assessment of system-level effects on module performance**
   Investigate how system design aspects, such as high string voltages (1500 Vdc), shading conditions, and bifacial module operation in roof top systems, affect long-term performance and reliability.
4. **Development of advanced diagnostic tools for PV monitoring**
   Design and validate an automated Dark I-V monitoring system capable of detecting electrical faults and degradation mechanisms in PV strings during nighttime operation.
5. **Establishment of a long-term monitoring platform**
   To create a reference PV installation with high-resolution monitoring that will enable long-term studies of module degradation, system performance, and reliability beyond the duration of the project.

Together, these objectives aim to improve the understanding of modern PV technologies in real operating environments and provide a scientific basis for future reliability studies and system design improvements.

3 Activities and Results

Chapter 3 describes the system design, monitoring infrastructure, laboratory characterization, and first performance and reliability results obtained from the RACONT2050 installations.

3.1 Module technology selection

The initial phase of the project focused on selection of suitable PV module technologies. One of the key objectives of the project was the investigation of high-voltage PV strings, where the selection criteria prioritised monofacial high-power modules (>500 W) and high-efficiency technologies (>21%) certified for 1500 Vdc system voltages. The original intention to restrict the selection to monofacial modules proved difficult due to the clear industry trend towards bifacial architectures in high-power PV modules. Given this market situation and the expectation that bifacial technologies will dominate future PV markets with increasing adoption also in residential systems, the study was expanded to include both monofacial and bifacial modules to enable a broader technological comparison.

Seven commercially available module technologies from five leading global manufacturers were selected. The manufacturers are anonymized in this report (referred to as Manufacturer A–E). Two manufacturers are represented by both monofacial and bifacial variants, resulting in seven module technologies in total. The selected modules represent industrial production technologies available at the time of procurement providing a snapshot of the market as of 2022. At that time, PERC technology was still widely deployed and commercially relevant. Since then, TOPCon has largely replaced PERC in many new high-efficiency module production lines. Nevertheless, the data collected in this project are highly valuable, as they provide a reference dataset for comparing the performance and behaviour of different technology generations under identical real-world operating conditions.

Table 2 presents the main datasheet parameters of the seven module technologies selected for RACONT2050.

Table 2: *PV technologies and main manufacturer data from datasheets.*

Tech	Brand	Cell technology	P_{nom} [Wp]	Bifaciality [%]	Module efficiency [%]	Pm temp. coeff. [%/°C]	**Warranty**	
							1st year Pm degrad. [%]	Annual Pm degrad. [%]
#1	**A**	PERC monofacial	540		21.1	-0.35	-2	-0.55
#2	**B**	PERC bifacial shingled	660	70±5%	21.2	-0.34	-2	-0.45
#3	**C1**	TOPCon n-type monofacial	560		21.7	-0.30	-1	-0.40
#4	**C2**	TOPCon n-type bifacial	560	80±5%	21.7	-0.30	-1	-0.40
#5	**D**	HJT bifacial	375	90±2%	20.9	-0.26	-1	-0.20
#6	**E1**	PERC monofacial	655		21.1	-0.34	-2	-0.55
#7	**E2**	TOPCon n-type bifacial	560	80±5%	21.7	-0.30	-1	-0.40

The nominal power ranges from 540-660 W, with module efficiencies between 20.9% and 21.7%. The modules fall within the median power class of each manufacturer's product portfolio. The technology-dependent bifaciality coefficient ranges from 70% to 90%, with the lowest values for PERC and the highest for HJT, indicating the ratio between rear-side and front-side power generation. Differences in the warranted degradation rates are also reported. It can be observed that compared to a few years ago, manufacturers have reduced the declared annual degradation rates from typical values of –0.7%

to –0.8% per year to –0.2% to –0.55% per year. TOPCon and HJT technologies specify lower long-term degradation compared to PERC modules.

The selected modules represent a range of state-of-the-art photovoltaic cell architectures and interconnection approaches. The selection was carried out considering not only the technological advantages of these innovations, but also the potential risks associated with recently introduced PV technologies, as summarised in Table 1.

- PERC technology with gallium-doped silicon wafers to mitigate light-induced degradation (LID), combined with multi-busbar interconnections and large M10 half-cut cells.
- Shingled monocrystalline-PERC bifacial glass-glass modules, where cells are electrically connected using low-temperature conductive adhesive bonding. This configuration reduces inactive area caused by ribbons and therefore lowers optical losses.
- n-type TOPCon modules, available in both monofacial (glass-backsheet) and bifacial (glass-glass) variants, using interconnections with circular tiling ribbons to reduce resistive losses and shading.
- Heterojunction (HJT) bifacial glass-glass modules, employing smart-wire interconnection technology with a large number of thin wires to improve current collection and reduce mechanical stress.
- Use of large PERC and TOPCon wafers (M10 and G12) to maximise power output through increased cell area and current.

In addition, several common design approaches are implemented across the selected modules:

- Half-cut cells, used in most technologies, reduce resistive losses, improve tolerance to partial shading, and enhance resistance to microcracks.
- Large wafer formats (M10 or G12) are adopted by most modules to increase module power output. Only the heterojunction modules use the smaller M6 wafer format.
- Advanced interconnection technologies, including MBB, SMBB, shingled cells and smart-wire, are applied to reduce ribbon shading and ohmic losses, improving module efficiency and reliability.
- Larger module dimensions (up to 2256-2384 mm x 1133-1303 mm, 540-660 W) compared to standard modules (~1650–1800 × 990–1050 mm, 400–550 W), enabling higher power (540-660W).
- Use of 2+2 mm thin glass for bifacial (G/G) modules compared to 3.2 mm glass for (G/B) modules.

The selected modules therefore represent different technological pathways currently pursued by the PV industry, enabling an evaluation of their relative performance under real residential installation constraints.

3.2 PV system Design and Construction

3.2.1 System configuration (Campus Viganello)

Roof configuration

To demonstrate and evaluate the performance of multiple technologies at a realistic (commercial) scale, space was needed to install at least 120 kW of PV modules. In the context of Switzerland, where flat land is at a premium, a rooftop installation was therefore most appropriate, which further needed to be easily accessible for scientific monitoring activities. Another important requirement for choosing the location for the RACONT Viganello system comes from experience with the 1982 TISO-10 plant: the

monitoring system had to operate, remain available and be maintained over a long period (30 years and more) beyond the initial funding of the project.

After an in-depth search, it was decided to use the roofs of the Campus EST USI-SUPSI at Viganello (Figure 1). Although the two available flat roofs are not completely free of technical elements, they have allowed the installation of 132 kW of PV modules, composed of seven technologies from five different module manufacturers. Moreover, the building management information system at the campus allowed for the inclusion of the RACONT plant data acquisition system, ensuring its long-term maintenance and data capture in line with the project objectives.

The flat roofs at Viganello consist of green roofs, allowing vegetation to grow and requiring additional maintenance for optimal system performance. Further constraints are the roof orientations (6-7 degrees West of South, which can cause more row-to-row shading in winter compared to an identical system oriented due South), and the presence of building technical elements on the roof, which can cause local shading, as well as limit array placement. As a consequence, the arrays of the RACONT system do not have identical row-to-row distances, with unequal row-to-row shading throughout the day and year (see chapter 3.2.2).

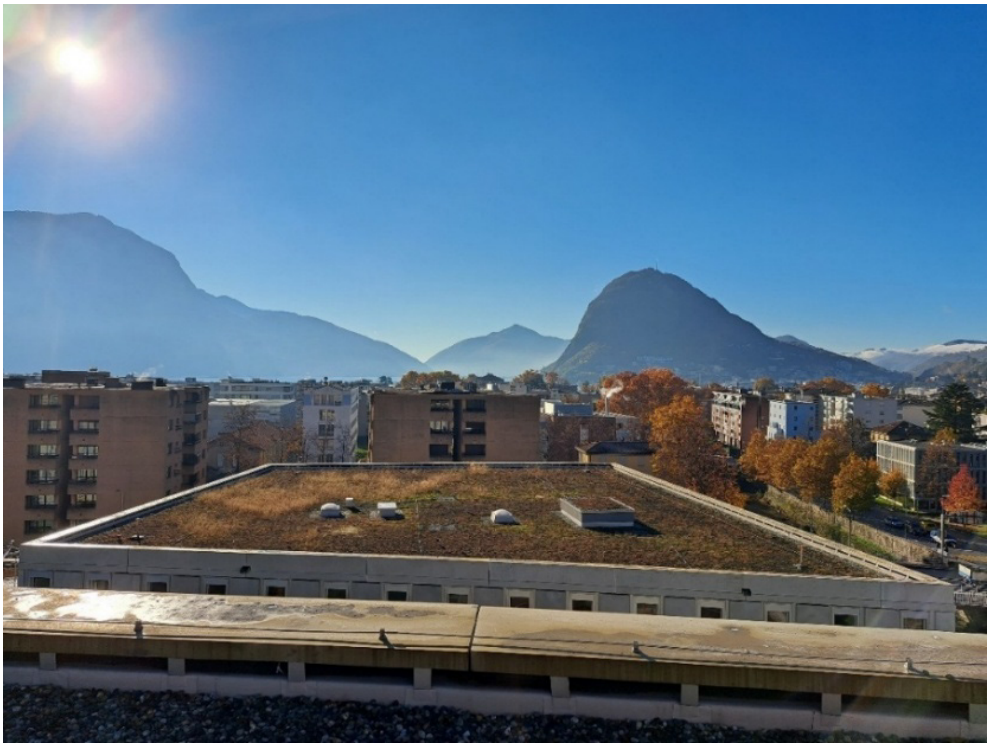

Figure 1: *View of the South roof looking West, from the USI/SUPSI building to the East, before the PV system was installed. Note the objects on the roof which constrain the degrees of freedom for array placements. The building from where the photograph was taken causes shading of the South roof.*

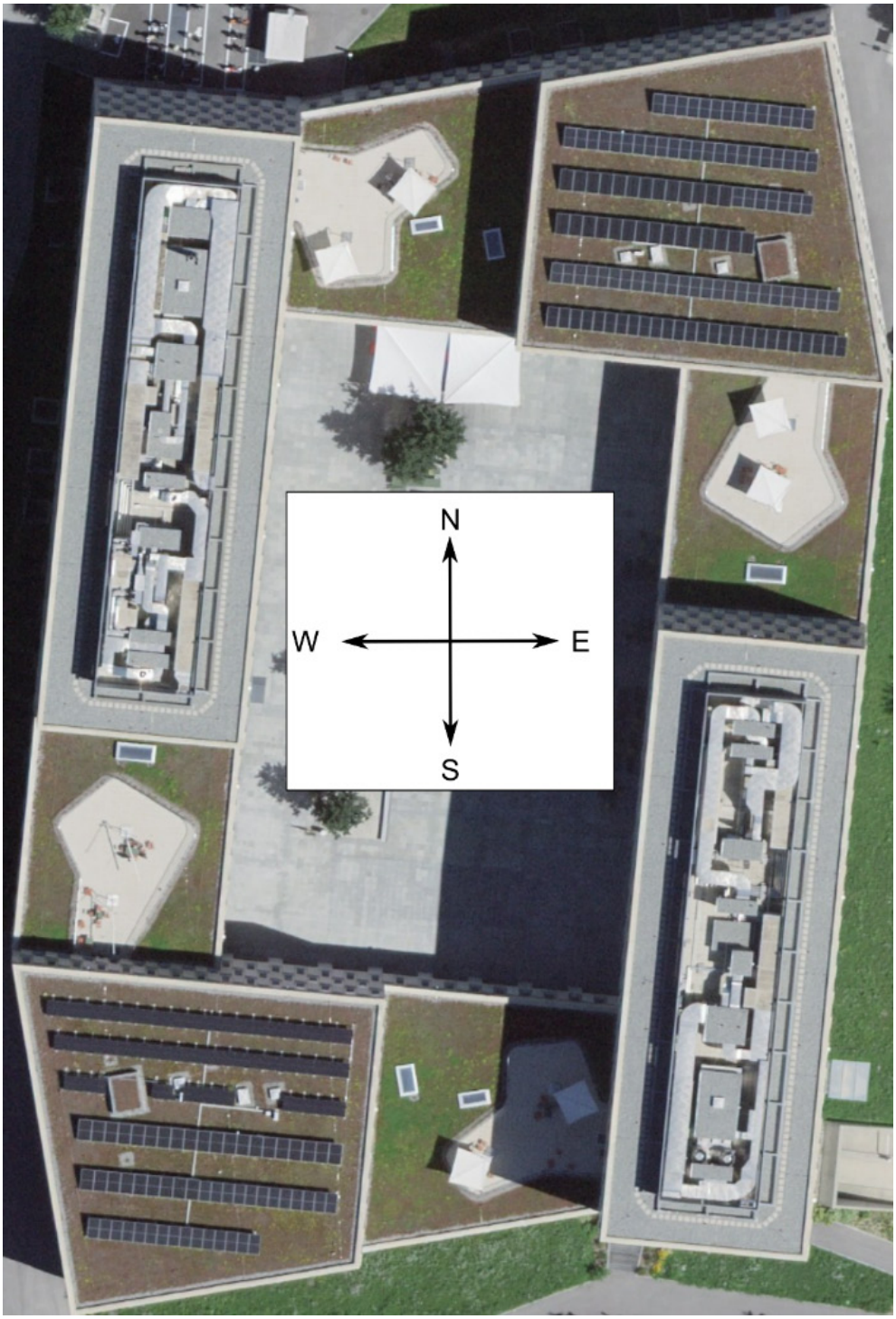

Figure 2: *Bird's eye view of the RACONT 2050 PV systems in Viganello. The South tower roof sees early-morning shading from the building on the right (East), while the North tower roof sees late afternoon/evening shading from the building to its left (West). Further irradiance losses on the arrays are from far shading from surrounding mountains, such as Monte Brè.*

Mounting structure configuration

Originally, the system was designed with a ground clearance of 70 cm. Due to regulatory and permitting constraints, the installation height had to be reduced to 32 cm. As this was late in the project and procurement phase, the final mounting system (see Figure 3) could not be specifically adapted to bifacial modules. Consequently, bifacial modules do not achieve their full yield potential. In addition, the installation on a green roof results in low and spatially inhomogeneous ground reflectance (albedo), which further limits rear-side irradiance. No dedicated construction was made for the bifacial modules, and the same fixing system was used for all module types. While these conditions limit the achievable bifacial contribution, they reflect realistic installation constraints commonly encountered in residential rooftop applications. The setup therefore provides the opportunity to study the behaviour of different module technologies under real operating conditions. The installation conditions will be taken into account when interpreting and comparing the measured module performances, particularly with respect to the bifacial contribution.

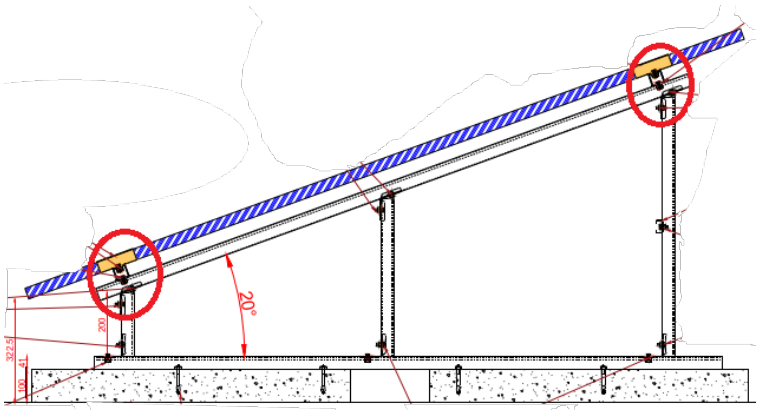

Figure 3: *The custom mounting structure used for the RACONT Viganello arrays.*

The mounting structures were built by the USI/SUPSI consortium responsible for the construction of the new Campus EST in Viganello, as no commercial options or suppliers were willing or capable of accommodating these module sizes. This reflects the difference in innovation speed between module manufacturers and racking/mounting system suppliers, and remains a risk for investors and procurement while module sizes and formats continue to rapidly evolve.

String configuration

Until recently, the standard system voltage of PV modules was 1000 Vdc. The system voltage in the new modules has increased to 1500 Vdc, initially only for PV modules intended for utility-scale or commercial & industrial (C&I) applications, but more recently also for residential applications.

While the higher voltage reduces current-related conduction losses, it increases the potential of the PV modules in a string to the earth, and with it the risk of PID. To evaluate this, high-voltage strings have been installed on each roof, one for each type of technology. Some technologies have multiple strings for a total of 10 strings distributed over the two roofs (five strings for each inverter). The final system configurations are shown in Table 3 and the string plan for each roof in Figure 4.

Table 3: *String, power and technology allocation by roof at Viganello. The short-circuit current under STC conditions Isc,STC is important for inverter current rating, while the open-circuit voltage Voc of the string must be below the module and inverter insulation limit of 1500 Vdc.*

Roof	MPPT #	Brand	Type	Cell tech	n°	Pnom module [W]	Pnom string [kW]	Isc string [A]	Voc string [V]
North	1	A	Mono	PERC	25	540	13.5	13.85	1237.5
	2	A	Mono	PERC	18	540	9.72	13.85	891.0
	3	B	Bifi	PERC	28	660	18.48	18.06	1313.2
	4	C1	Mono	TOPCon	25	560	14.00	14.15	1261.8
	5	C2	Bifi	TOPCon	26	560	14.56	14.13	1317.4
	Total or average				**123**	**572**	**70.26**	**13.94**	**1204.2**
South	**MPPT #**	**Brand**	**Type**	**Cell tech**	**n°**	**Pnom module [W]**	**Pnom string [kW]**	**Isc string [A]**	**Voc string [V]**
	1	D	Bifi	HJT	30	375	11.25	10.4	1338
	2	D	Bifi	HJT	23	375	8.63	10.4	1025.8
	3	D	Bifi	HJT	21	375	7.88	10.4	936.6
	4	E1	Mono	PERC	29	655	19.00	18.43	1313.1
	5	E2	Bifi	TOPCon	27	560	15.12	13.93	1363.5
	Total or average				**129**	**468**	**61.88**	**12.05**	**1195.4**

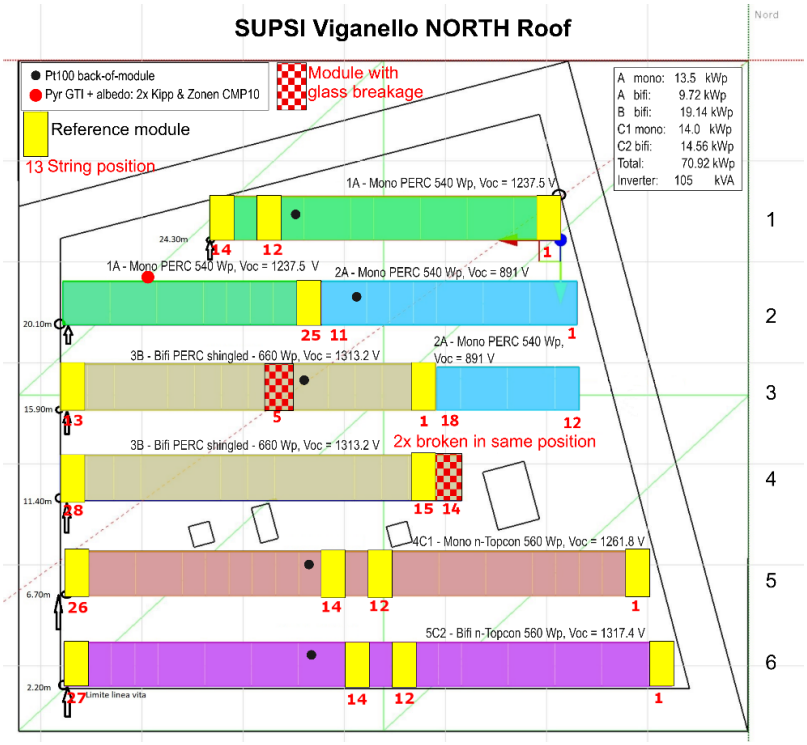

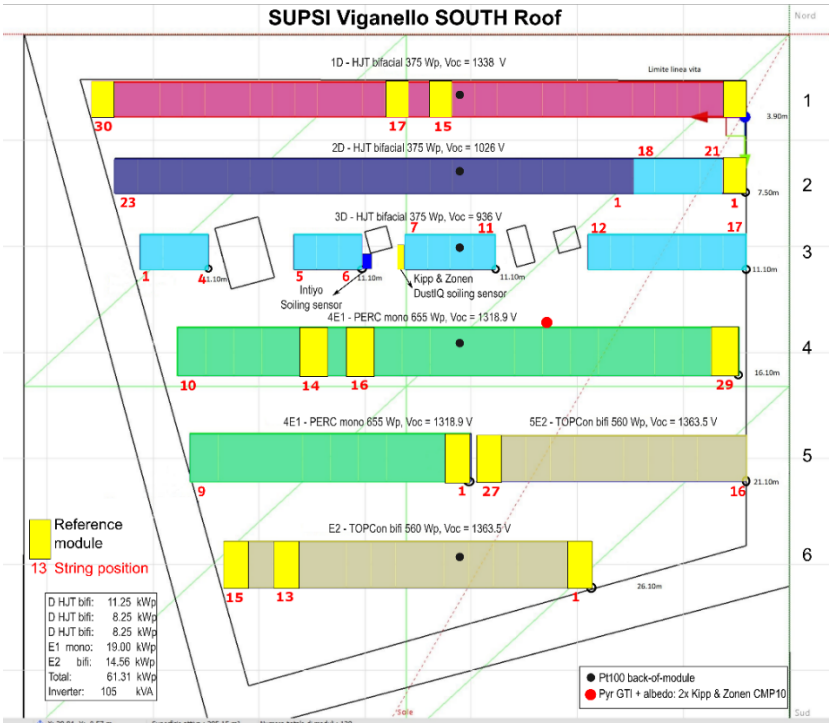

Figure 4: *Arrangement of strings on the roofs at Viganello, with sensor placements and location of reference modules for each technology. Modules with glass breakage are also indicated.*

Inverter choice

Low to medium power inverters (<50 kW) available on the market have input voltages in the range of 800 Vdc to 1100 Vdc, while 1500 Vdc ratings are generally associated with higher power ratings (>100 kW). Recent design changes to PV modules have lowered the open-circuit and maximum power point (MPP) voltage per module, allowing for longer strings. At the same time, module currents have increased significantly. While typical short-circuit currents were previously in the range of 8 A to 10 A, some of the RACONT modules reach short-circuit currents of up to 18 A (see Table 3). As current losses in conductors scale quadratically (Ploss = I^2*R), this affects protection fuses, inverter ratings, as well as bypass diodes in modules. Any (localised) increase in resistance R, e.g. due to a bad soldering contact or small deviation in a bypass diode, can then encounter much higher power than historical design experience, and therefore new failure points in PV systems. Longer strings are possible and desirable in ground-mounted conditions, while space and module installation (tilt and azimuth) constraints become more challenging in roof-mounted systems. This is evident in Figure 4, where strings have to run over two arrays to achieve the desired string voltages to be tested.

The only inverter which came closest to the required characteristics and provided 1500 Vdc strings was a Huawei SUN2000-105KTL-H1. The total inverter power (105 kW) exceeds the DC power on each roof, resulting in a low DC:AC ratio (0.58 for the South tower, and 0.675 for North), while typical design practices see DC:AC ratios in the range of 1.2 to 1.5, with the aim to improve inverter efficiency, and to compensate for temperature losses, and future module degradation. This inverter has 6 independent MPPTs (only five are used, given the space constraints for the strings), which allow separate operation and monitoring of each string with the required max input current (up to 18 A).

String polarisation

PID is a degradation mode induced by a high voltage stress of the module frame to ground. The occurrence of this failure depends on the magnitude of the voltage (number of serially connected PV modules per string) and the polarity of the electrical field build-up between the framing/glass surface and the solar cells. The overall string voltage is distributed among all individual PV modules within a string. How this voltage distribution happens depends on the inverter type used. For example, in the case of a 1200 Vdc system in a transformer less inverter, typically the voltage is symmetrically distributed with respect to the earth, -600 V and +600 V. It is common to have an offset more in the negative side (for example, -700 V and +500 V).

To understand the string polarisation within the RACONT systems, measurements were taken on the two inverters located in Viganello. Figure 5 and Figure 6 shows up to 17% non-symmetrical polarisation to ground (a negative offset) for high voltage strings. These values indicate a non-uniform distribution of voltages with respect to ground, and therefore the potential for non-uniform PID occurring throughout the strings. Depending on its position within the string and the voltage it sees, a module may be affected differently by PID. For this reason, for each technology and string reference modules are selected: two are positioned at the ends of the strings, while two others are installed in the middle section (see Figure 4). These reference modules will be removed and analysed in regular intervals of 1-2 years to check whether the modules are subject to greater degradation than the reference modules in the low-voltage strings at the Trevano Campus (see section 3.2.2).

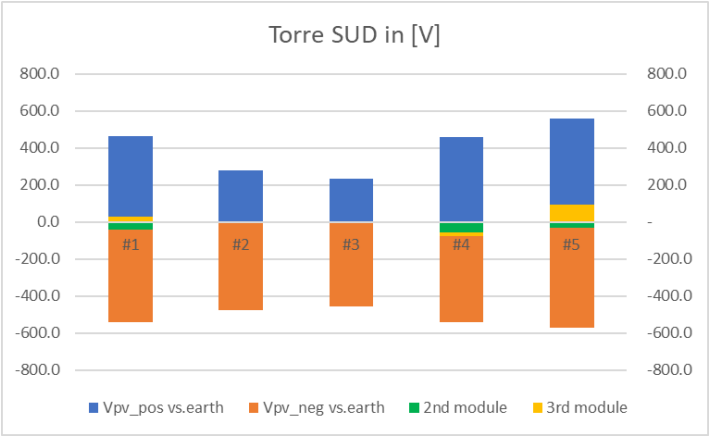

Figure 5: *Measured distribution of voltages towards ground in strings of the South Tower.*

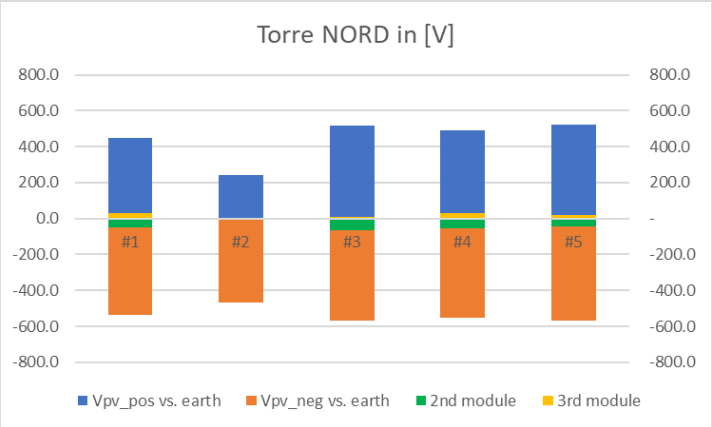

Figure 6: *Measured distribution of voltages towards ground in strings of the North Tower.*

3.2.2 System configuration (Campus Trevano)

During 2023, a second installation with low-voltage strings of 6 modules each, was built on the roof of the Aula Magna in Trevano (see Figure 7), adjacent to the remaining 1982 TISO installation. Due to the lack of roof space, and availability of modules, only five technologies (out of seven) could be installed. The total power of the low voltage RACONT PV system is 16.74 kWp.

Compared to the Viganello Campus installation, the Trevano roof is covered by a layer of gravel and therefore with a different albedo. The bifacial technologies benefit less than at Viganello, due to the low ground clearance, while the tilt angle is the same.

Figure 7: *Five new technologies were installed near the 40+ years old PV system TISO on Aula Magna roof in Campus Trevano.*

Table 4 shows the string configuration at Trevano, including the old TISO-10 modules and the 5 Viganello module technologies. The old TISO-10 PV system installed in 1982 has 48 functioning modules divided into 4 strings of 12 ARCO Solar ASI 16-2300 (35 W) modules, with a total (initial) nameplate power of 1.6 kW.

The Table highlights the impressive technology improvements of the PV industry over the past 40+ years: the TISO Arco Solar modules had a total module efficiency of 10%, and a module area of 0.37 m² [8]. By contrast, the RACONT modules have 10 to 19 times the nominal power, thanks to module efficiencies more than doubling to ~21%, and module areas increasing to 2-2.5 m² (6 to 8 times the Arco Solar module area).

Table 4: *Modules and strings installed at Trevano, next to the TISO-10 system with Arco Solar modules. Inverter and MPPT string numbering correspond to the placement seen in Figure 7.*

Inv-MPPT #	Brand	Type	Cell tech	n°	Pnom module [W]	Pnom string [kW]	Voc String [V]
4-2	E1	Mono	PERC	6	655	3.93	271.7
4-1	C2	Bifi	TOPCon	6	560	3.36	304.0
3	D	Bifi	HJT	6	375	2.25	267.6
1-2	A	Mono	PERC	6	540	3.24	297.0
1-1	B	Bifi	PERC	6	660	3.96	281.4
2	ARCO	Mono	Al-BSF	48	35	1.60	200.0
Total or average, excluding TISO				**30**	**572**	**16.74**	**284.34**

Finding residential-scale inverters rated to deal with the high input current from the project's modules was a challenge. Consequently, two inverters with two MPPTs and a small inverter for the string with the least power (D-3, see Table 4) were chosen. The inverters are all located on the roof at a short distance from the strings, minimising cable losses.

The old TISO data acquisition system has been adapted and updated so that the new strings with higher currents can be adequately measured. A new datalogger has been installed and connected to the SUPSI servers. Data from Trevano are acquired since November 2023.

3.3 Monitoring system

3.3.1 String monitoring solutions

The PV data acquisition system was integrated into the Siemens domotic system of the Viganello Campus, which helps ensure the longevity of the data capture to 2050 and beyond. The main parameters such as string-level DC data (voltage and current), AC parameters (E, P, Vac, Iac, etc.), inverter measurement data (DC and AC values, e.g. string currents and voltages (DC), and AC power, frequency, etc) and weather parameters (irradiance, albedo, temperatures) and soiling measurement system are measured, see Figure 8. An alarm system on the functionality of the power plant was implemented in the domotic system, to meet PV system grid connection requirements [14]. All data are saved on the SUPSI ISAAC data server. A Grafana dashboard is connected to the database, allowing for rapid visualization and analyses to be done, as well as generating monitoring alarms.

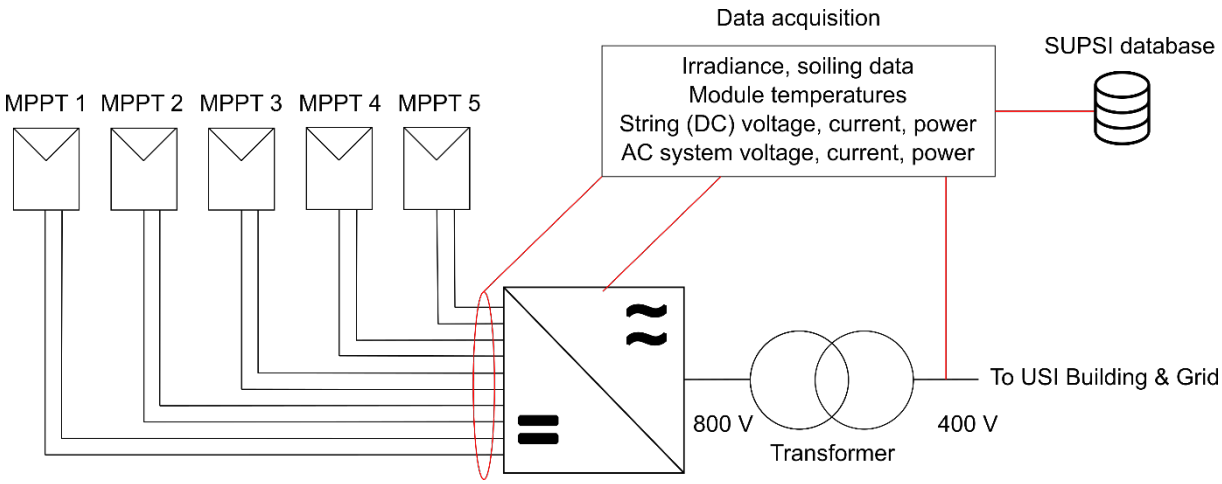

Figure 8: *Monitoring schematic at Viganello for both roofs. The South tower has two soiling sensors installed, the North tower has none. Each inverter has 5 MPPT inputs in use, one per string.*

3.3.2 Dark I-V string monitoring system

While long-term monitoring of key performance indicators (KPIs) can provide insights into the yield and performance of a plant, it does not offer a detailed analysis of possible defects in PV strings and modules. Traditional on-site evaluation techniques, such as daylight I-V measurements, thermography, and electroluminescence, are highly weather-dependent and time-consuming. By contrast, dark (reverse) I-V measurements can be done at night, and are therefore much less weather-dependent, while providing similar insights to the previously mentioned techniques to evaluate the health of a system, such as series resistance, parallel resistance (as well as PID, LeTID), and shorted bypass

diodes. The IEA PVPS Task 13 report 'Qualification of Photovoltaic (PV) Power Plants using Mobile Test Equipment' [15] gives a detailed overview about field inspection techniques and commercial products, including measuring I-V curves in the dark.

To measure the I-V curve of a PV module or string at night, the measuring device must provide sufficient power and bias the module or string enough for a voltage sweep to be done: for a 1500 Vdc string, the measurement device should provide a voltage of 1700-2000 Vdc. As the power and voltage of strings increase, so do the requirements for dark I-V curve measurement devices. To date, no commercially available dark I-V measurement devices can measure PV strings up to 1500 Vdc and handle high module currents (18 A to 20 A at short-circuit conditions). The only commercially available dark I-V measurement devices on the market today (after the end of the RACONT project) measure 1500 Vdc, 10 A.

To track performance and detect possible faults in PV systems, an automatic monitoring system that measures the dark I-V characteristics at night was developed within RACONT. The goal of these in-situ dark I-V measurements is to demonstrate the possibility of detecting failures such as bypass diode failures, string-level PID, increased series resistance, and electrical mismatches between strings, in real-time or much faster than through punctual field inspections

The design and implementation of the in-situ dark I-V measurement system had some technical and budgetary constraints. High-voltage generators have the drawback that they cannot provide the required voltage and current without a ripple in the signal (a type of undesired noise, which would affect measurements and their interpretation). Moreover, the costs of such generators in this voltage, current, and power range were beyond the available budget.

The decision was therefore made to build a linear regulator of the sweep ramp, based on a high-voltage capacitor pack for energy storage, with the capacitor pack charged using a flyback converter. The realisation of a prototype of a "Dark I-V Measurement System" (DIVMS) was the subject of a semester's work (2023) and a student's final master's thesis in electronics (SUPSI-DTI; 2024).

Before implementing the hardware prototype, circuit simulations were carried out to evaluate the behaviour of the measurement system.

Simulation of dark I-V measurement

The inherent capacitance of high-efficiency PV modules (e.g., PERC, TOPCon, HJT) influences the accuracy of dark I-V measurement, and therefore determines the minimum voltage sweep time of the dark I-V measurements: the measurements must be done slow enough for the capacitive effect of the PV modules to have a negligible effect. High-voltage capacitor packs must therefore contain sufficient energy to power the high-voltage PV string. In addition, the length and arrangement of the connecting cables influence the parasitic inductances and thus the measurements.

To design the measurement system, initial circuit simulations were performed using PLECS, a software designed specifically for power electronics applications. A single diode model was introduced with some adjustments to consider all conditions and account for any parasitic capacitance in modern PV modules and inductances in cables. All seven technologies were implemented with estimated capacitances.

Figure 9 presents the results of these simulations, providing insights into the relationship between measurement speed and accuracy.

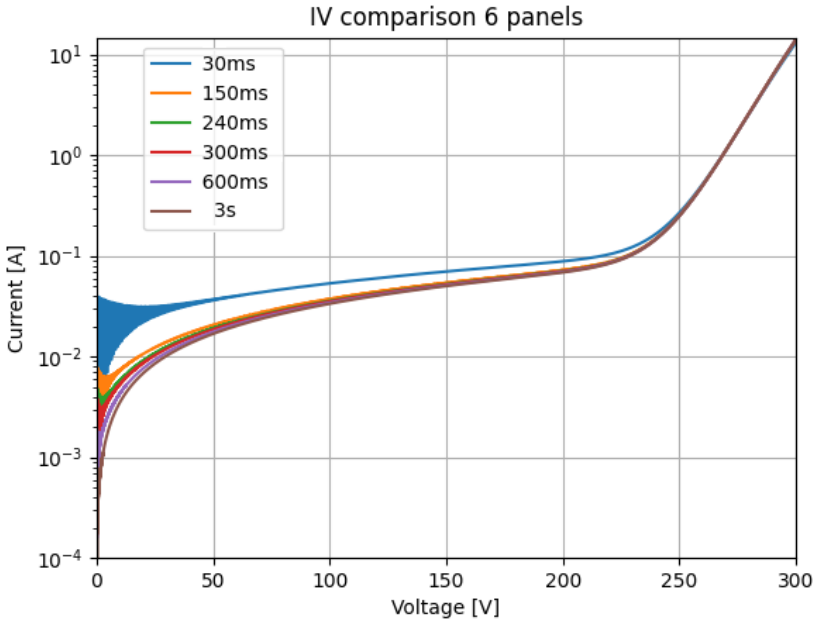

Figure 9: *Simulation of the dark I-V curve for the same 6-module string at different measurement speeds, showing the capacitive effect of high-efficiency modules during I-V curve measurements. 30 ms is clearly too fast, as seen in the large deviation to the other measurement durations.*

The relationship between measurement speed and accuracy also varies with the number of modules in the string, making it difficult to present an exact figure for the minimum time required to accurately acquire the I-V curve. A time of approximately 300 ms gives a good balance between accuracy, power and energy required, and flexibility with varying string lengths.

Other simulations were conducted to better visualize the impact of series and shunt resistance (Rs and Rsh) changes in PV modules. Figure 10 (a) and (b) show the results on a single module.

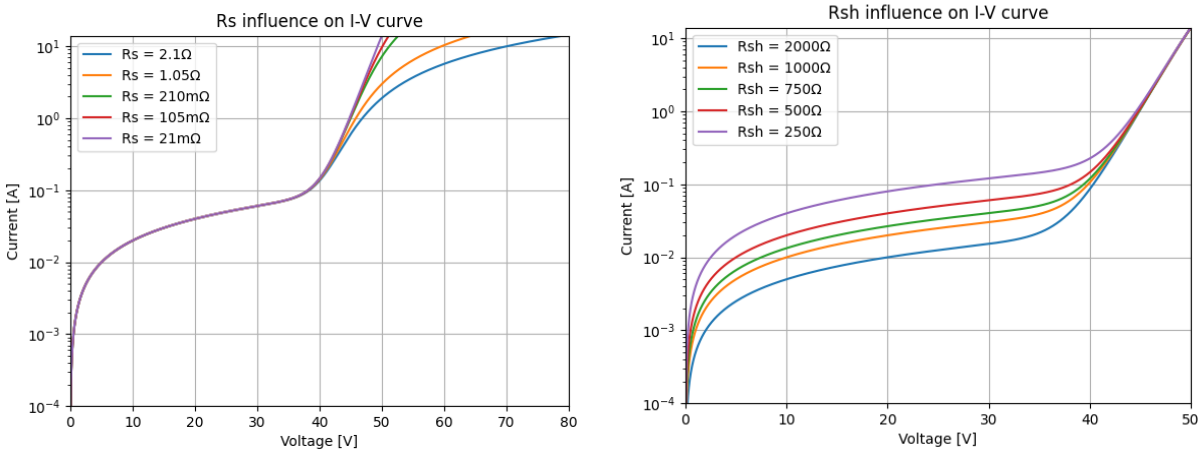

Figure 10: *(a) Series resistance Rs influence on simulated dark I-V curves and (b) Shunt resistance Rsh influence on simulated dark I-V curves. The change in the series resistance leads to resonant behaviour, with the I-V curve exhibiting a clear jump in current for low Rs at ~40 V. The capacitance effect is noticeable in the large differences observed between 0 V and 40 V for varying Rsh values.*

The simulations show resonant behaviour and other capacitance effect (Figure 10). To avoid these behaviours a sectional ramp as shown in Figure 11 with two different slopes was introduced. The simulations carried out on a string of 30 modules of Tech #2, with Isc =18 A, with two different slope speeds combined with each other and at different voltages shows the suppression of resonance problems. The inductance of the cables did not give any noticeable problems.

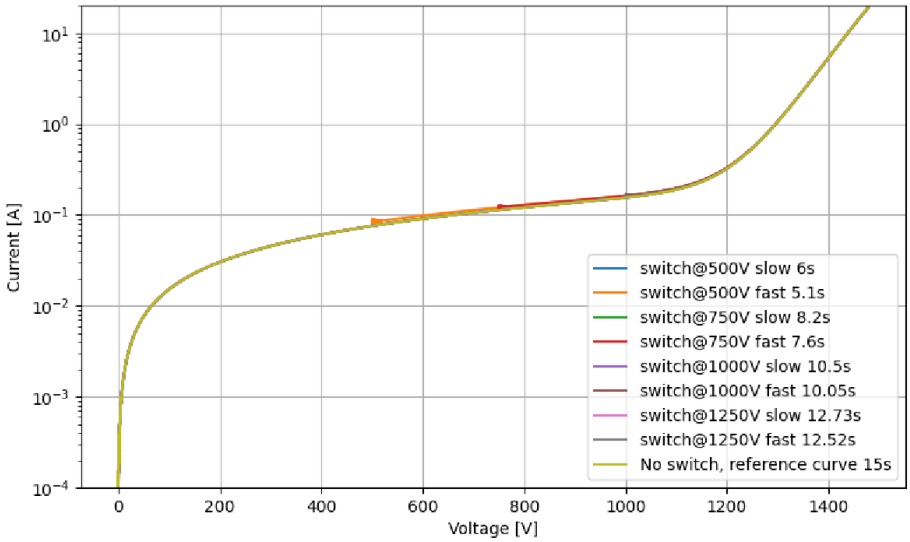

Figure 11: *Simulation of dark I-V string of 30 Tech#2 PV modules in series, and Voltages up to 1250 V.*

Depending on the speed of the ramp in the various portions of the curve, the measurement accuracy is affected as well as the energy consumed. A compromise was therefore sought between a speed slow enough to limit measurement errors and a speed fast enough to limit the energy required for measurement and thus the size (and cost) of the capacitors. The energy needed for a balanced sweep of a 1500 Vdc string is approximately 2100 J, or 0.58 Wh, i.e. very low compared to the energy production of the string in one day.

Design of the dark I-V system

To trace the I-V curve of a 1500 Vdc, 20 A string in 300 ms, approximately 2.1 kJ of energy is required. Given the need for rapid energy release during the measurement, capacitors are used for energy storage.

As the I-V curve is traced, the voltage applied to the PV string gradually increases from 0 V to 1500 V. The energy storage system must be able to maintain this voltage until the end of the measurement. However, as the energy is supplied, the capacitors discharge, causing their voltage to decrease. This means the initial stored voltage must exceed 1500 V to ensure sufficient voltage at the end of the measurement. To achieve this within the 300 ms measurement time, a charging voltage of 2000 V and a capacitance of 2400 µF (three 800 µF capacitors in parallel) is needed.

The high voltage to charge the capacitor bank is generated using an isolated AC/DC converter, employing a current-mode flyback topology that operates in either critical conduction mode (CrCM) or discontinuous conduction mode (DCM), depending on the voltage of the capacitor bank: the capacitor bank current load is highly dynamic (it follows a typical RC-network charging shape). At the start of the charging process, CrCM is better and more efficient at transferring large currents (and therefore charging) to the capacitor bank. As the capacitor charges, its voltage increases, and the current (and charge) that can be transferred decreases: at this point, DCM is more advantageous and prevents over-

charging the capacitor, which can lead to catastrophic failure. The key here is that using these two modes ensures reliability, efficiency and safety of the charging operation of the capacitor bank. The disadvantage is that the design and control of the flyback converter is more complicated, as two conduction modes must be programmed to ensure a smooth transition from one to the next.

The voltage from the flyback converter can be regulated according to the string voltage (Voc at the actual module temperature measured), up to a maximum of 2000 V, ensuring that only the energy required to trace the I-V curve is stored, which further improves system efficiency.

To trace the dark I-V curve, a linear regulator utilizing insulated gate bipolar transistor (IGBT) transistors was developed to control the current flowing through the PV string during measurements.

To achieve accurate voltage measurement with high resolution across the wide range of 0 V to 1500 V in the PV string, a differential measurement technique is employed with auto-range management. Similarly, high precision current measurement across the wide current range is achieved with auto-range amplifiers and three shunt resistors in series.

The conditioned signals are then fed into an analogue-to-digital converter (ADC) for simultaneous sampling and then to a microcontroller with the calibration parameters. This approach ensures a very high level of accuracy and precision of measurements in all ranges.

Preliminary tests

To test the developed DIVMS, a high-voltage string (977 Vdc) of modules was assembled using 26 damaged PV modules TSM-260PC05A at SUPSI PVlab. These modules were obtained from a solar plant that was decommissioned after the 2023 hailstorm near Locarno (TI). This string of damaged modules thus presented an excellent opportunity to use the dark I-V measurement system for which this technique is most suitable: identifying issues, such as degradation (visible in changes to Rs and Rsh), or bypass diode problems.

The DIVMS is directly connected to the string of modules using a 4-wire configuration, or a single module at a time. The modules are stacked on top of each other and are covered with a black blanket to guarantee night conditions (see Figure 12). This also illustrates the benefit of dark I-V measurement for rapid and scalable detection of issues, as it can be performed in a limited space, compared to illuminated I-V curve measurements.

Figure 12: *Dark I-V measurement set-up at SUPSI Mendrisio campus*

The goal of these preliminary tests was to evaluate each module individually for comparative analysis and then to emulate a string of 26 damaged modules in series with extra shunt and series resistances. One of the 26 modules had glass damage, while the other modules only had damaged cells (microcracks) from the hailstorm they experienced.

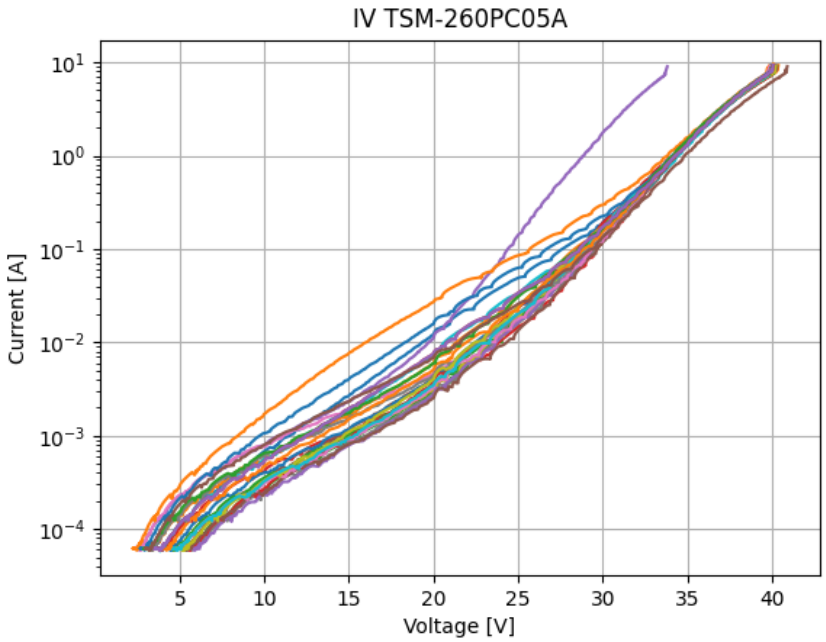

Figure 13: *Comparison of the measured dark I-V curves for individual modules of the 26 TSM modules following a hailstorm. The large spread in values at lower voltages indicates Rsh variations, whereas deviations at higher voltages indicates Rs variations.*

As shown in Figure 13, the modules sustained unequal damage, resulting in varied dark I-V characteristics. The most affected parameter by the damage was the shunt resistance (large spread in values at lower voltages in Figure 13). However, in some cases (see purple curve in Figure 13), the series resistance was also notably impacted, causing higher losses under high irradiance conditions.

Subsequent measurements were conducted on a string composed of the 26 damaged modules connected in series. These tests were designed to evaluate the increase in power and the DIVMS's performance for its intended purpose of measuring PV strings. Three tests were performed in the lab, the results are shown in Figure 14 and Figure 15.

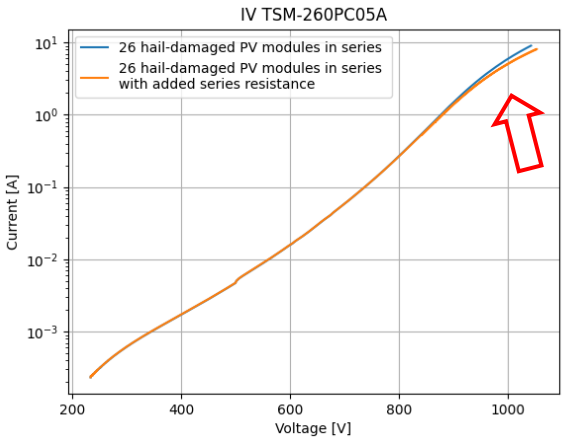

Figure 14: *Comparison of the dark I-V curve of 26 hail-damaged PV modules with and without an added series resistance of 2.5 Ω.*

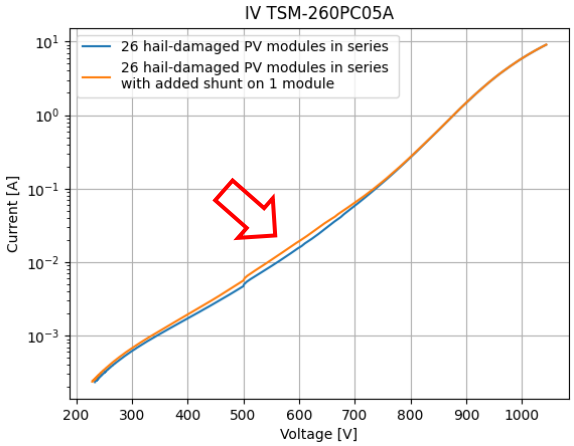

Figure 15: *Comparison of the measured dark I-V curves of 26 hail-damaged PV modules with and without added shunt resistance of 400 Ω.*

The first test involved measuring the I-V characteristic of the string in its existing condition with the damaged modules. The second test introduced an additional resistance of 2.5 Ω in series to the string, to emulate a series resistance fault (representing possible failure modes such as (large) cell cracks, delamination, or corrosion of busbars) using the initial measurement as a baseline. Finally, a third test involved inserting a shunt resistance of 400 Ω in parallel with a single module, while measuring the full string of 26 modules, simulating failures such as encapsulant degradation, potential-induced degradation, and microcracks. The parasitic series resistance of 2.5 Ω is easily detectable in the I-V characteristic (Figure 14), as is a parasitic resistance of 400 Ω in parallel to a single module (Figure 15). Identification of *which* module in the string suffers a shunt resistance issue is not possible using the string-level measurements, yet the string-level measurements are a good diagnostic tool to identify which strings have issues and subsequently analyse with other diagnostic tools.

The results clearly indicate that the designed DIVMS is able to detect even small variations in a large string and serves as a key starting point for subsequent in-depth failure detection. In practice, this means that first string-level dark I-V curve measurements can be used to detect any issues, compared to a one-diode equivalent model or neighbouring strings. Strings with issues can then be subjected to further analysis, such as electroluminescence (EL) to infrared thermography (IRT), or module-level dark and daylight I-V measurements. This also means that dark I-V measurements at the string level can reduce the testing and diagnostic work needed for a full plant, as it helps to identify problematic strings that merit further investigation and avoids the need to test the full plant, which is financially not useful.

3.3.3 Soiling monitoring sensors

Soiling of PV modules plays an important role in PV systems, reducing yield by blocking sunlight, while increasing hot-spots on modules and partial shading behaviours, thereby decreasing long-term system reliability. To increase system power and reduce wind loading, most flat roofs have a low module inclination angle between 10° and 15°. This relatively low inclination angle reduces the self-cleaning effect seen with higher inclination angles. In RACONT a slightly higher tilt angle of 20° was chosen to reduce soiling losses by favouring self-cleaning and further improve the energy yield of the bifacial modules. To limit row-to-row shading losses, the distance between the rows was increased.

During 2023, two devices for determining the soiling ratio of exposed modules were purchased and tested to track the self-cleaning effect of rain and possibly quantify the production loss due to the soiling. The soiling ratio is defined as the ratio between the impact on a soiled and a clean surface, which can be detected using different measurement principles. The standard IEC 61724-1 [16] allows different approaches to be applied, from evaluating the ratio of the short-circuit current of two reference cells (one cleaned, one untouched), to that of full modules (clean versus soiled), or the ratio of the power of these devices. Other permitted alternatives are to use optical principles, where the impact of soiling on a surface is determined using reflection or transmission of light. The soiling ratio and soiling loss are mathematically defined as follows:

$$Soiling\ ratio\ SR\ = \frac{I_{sc,dirty}}{I_{sc,clean}}\ or \frac{P_{m,dirty}}{P_{m,clean}}\ [\%]$$

$$Soiling\ loss\ SL\ = 1 - SR\ [\%]$$

The Kipp & Zonen DustIQ compares how well the glass surface reflects light back to the light-emitting sensor on two locations (the two circles visible on the DustIQ sensor of Figure 16) and computes a soiling ratio using a proprietary algorithm. The Intiyo sensor also uses a proprietary approach to calculate the soiling ratio, combining locally measured short-circuit current with data from other sources (e.g. satellite data). The Intiyo measurement system measures the plane-of-array irradiance through the short-circuit response of the PV cells in the sensor, and the temperature of the cell. The two soiling sensors were installed on the Viganello Campus South tower (see Figure 16).

Figure 16: *Soiling sensors installed: Intiyo sensor (left) and DustIQ Kipp&Zone sensor (right).*

The Intiyo comparison with the actual energy production and with the satellite irradiation data allows to evaluate in detail the operating status of the system. The output values are recorded separately and displayed by the server on Intiyo dashboard with data analytics, historical and real time performance assessments (see Figure 17). The Intiyo is a self-powered sensor and communicates via Wifi.

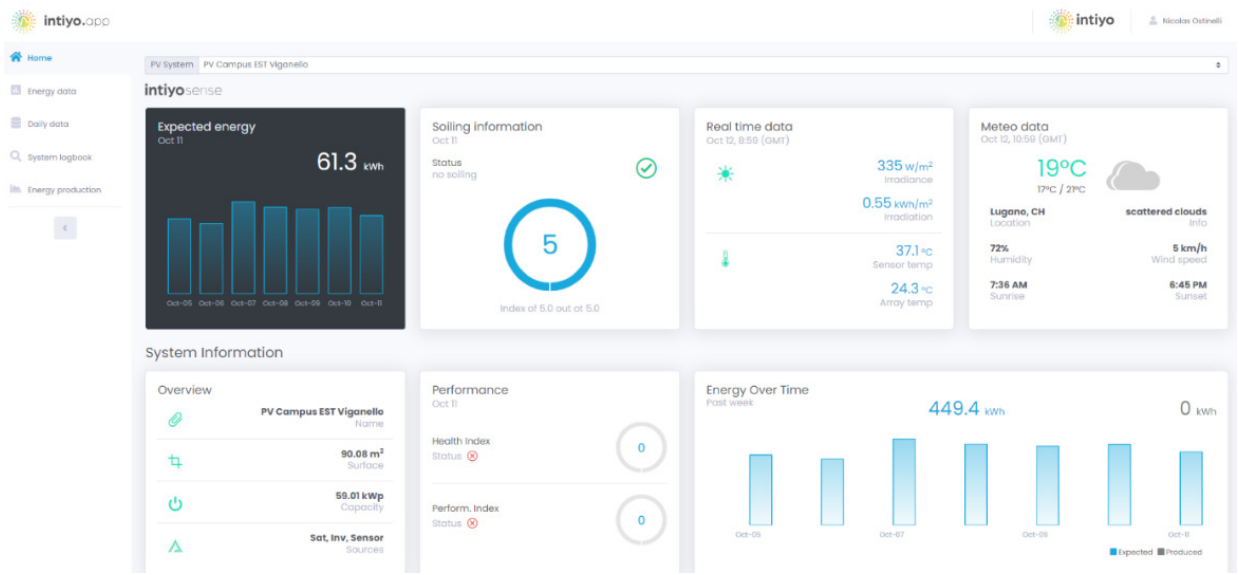

Figure 17: *Intiyo dashboard*

DustIQ from Kipp&Zonen, uses an Optical Soiling Measurement technology to measure the transmission loss of nearby PV modules due to soiling. It does not need sunlight to make measurements and updates every minute, night and day. The output values are recorded via RS-485 in the Siemens measurement system and with the API provided, data are imported into the InfluxDB database.

In Figure 18 an example is shown of a weather situation without rain for several days and consequent accumulation of dust on the sensor and on the modules. Heavy rains began on 6 July and continued through most of the day, causing the sensor and modules to be cleaned. In this case, soiling losses reached 1.6%, before the rain fully cleaned the modules and bringing the soiling loss to 0. (The soiling ratio would therefore have gone from 98.4% to 100%.)

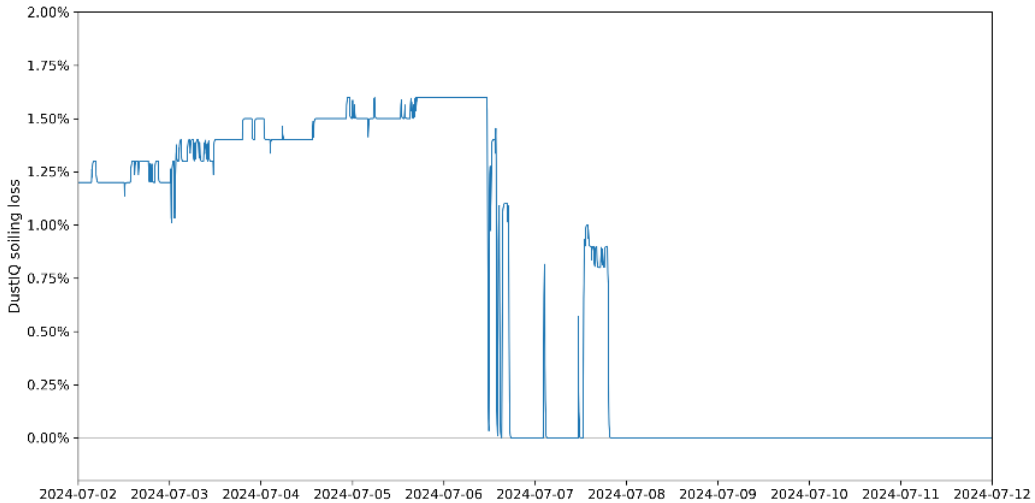

Figure 18: *Example of the trend of the soiling loss at Viganello measured with the DustIQ sensor*

3.4 Laboratory tests and field inspections

This chapter presents the results of the laboratory characterization and field inspections carried out on the photovoltaic modules installed on the RACONT systems. The objective of these tests is to assess the initial electrical performance of the modules, to measure the degradation of modules installed in the system and identify potential failure mechanisms affecting different module technologies.

The test program performed within the project, combines indoor laboratory measurements with field inspections. A set of reference modules for each technology were characterized in the laboratory before installation and subsequently re-measured after field operation. In parallel, regular visual inspections were conducted on all installed modules to detect early failures.

The collected data provide valuable insights into the early degradation behaviour of the investigated technologies and help identify potential reliability issues that may affect long-term system performance. An analysis of observed failures is presented.

3.4.1 Laboratory tests

Due to logistical constraints, it was not possible to measure the modules before installation of the Viganello system, as the modules had to be delivered directly to Viganello for installation, without the possibility of removing individual modules for laboratory characterization. The remaining modules were subsequently delivered to the laboratory for characterisation.

Four modules per technology were selected from these and installed in the Viganello system, replacing modules that had already been mounted during the construction of the system. Once installed, these modules will serve as field **reference modules**. The reference modules are removed every 1–2 years and measured in the laboratory to evaluate performance degradation occurring in the field. The reference modules are distributed along the string (see Figure 4), with one module installed at each end of the string and two modules placed in the middle to detect any difference in degradation due to PID.

The removed modules are instead stored in the laboratory and maintained either as dark reference modules (dark REF) or as spare modules to use in case of module damage.

The remaining tested modules were used to assemble the low-voltage string system installed at the Trevano site.

Test program

Prior to field installation, all reference modules underwent a light exposure of 10 kWh/m² under a steady-state sun simulator to quantify the **initial light-induced degradation (LID)**.

The following table illustrates an example of a complete test sequence, from the initial incoming inspection and laboratory measurements to the first control measurement carried out in October 2024.

Optical and electrical inspections consist of visual inspection (VI) and electroluminescence (EL) measurements, and respectively STC performance (PM) and low irradiance performance measurements (GCO). In case of bifacial modules, the rear side performance and bifaciality are also measured. The temperature coefficient could not be measured because the modules exceeded the size of the thermal chamber.

Table 5: *Example of the test sequence of a bifacial module technology. (Legend: VI (visual inspection), EL (electroluminescence), PM (performance @STC), GCO (performance at different irradiances), IN (insulation resistance), WL (wet leakage test), LS (light soaking), Bifi (bifaciality))*

Module / Locations	OUTDOOR REF										SPARE / DARK REF			
SUPSI Lable	**B1**	**B2**	**B3**	**B4**	**B5**	**B6**	**B7**	**B8**	**B9**	**B10**	**B11**	**B12**	**B13**	**B14**
Delivery	*delivered to PVLab and measured out of the box*										*delivered to Vigaenllo*			
Optical inspection	VI	VI	VI	VI	VI	VI	VI	VI	VI	VI	**Viganello** (10 months) 01.12.2022-27.09.2023			
	EL	EL	EL	EL	EL	EL	EL	EL	EL	EL				
Electrical performance tests (out of the box)	PM	PM	PM	PM	PM	PM	PM	PM	PM	PM				
	GCO	GCO	GCO	GCO	GCO	GCO	GCO	GCO	GCO	GCO				
Insulation resistance	IN				**Trevano** 27.10.2023-ongoing									
	WL													
Light soaking (intial stabilisation)	LS	LS	LS	LS										
Electrical performance tests	PM	PM	PM	PM										
	Bifi	Bifi												
Outdoor weathering	**Viganello** (13 months) 29.09.2023-22.10.2024													
Optical inspection	VI	VI	VI	VI							VI	VI	VI	VI
	EL	EL	EL	EL							EL	EL	EL	EL
Electrical performance tests	PM	PM	PM	PM							PM	PM	PM	PM
	GCO	GCO	GCO	GCO							GCO	GCO	GCO	GCO
Outdoor weathering	**Viganello** 11.11.2024-ongoing										**dark storage** 28.09.2023-ongoing			

Initial performance data with and without stabilisation

Table 6 presents the average electrical performance of all modules measured at STC, both in the out-of-the-box condition and after light soaking (LS) together with the deviation from the nominal and initial power, the so-called light-induced degradation. Examples of EL images for each technology are reported in the Annex.

Table 6: *Initial indoor measurement results of the 7 technologies as delivered (out of the box) and after 10 kWh/m² of LS.*

Brand (# mod)	**Type**	**P_{nom} [W]**	**avg. P_m [W]**	**ΔP_m [%]**	**avg. P_m [W]**	**$\Delta P_{m,avg}$ [%]**	**$\Delta P_{m,max}$ [%]**
		datasheet	*Out of the box*	*P_m vs. P_{nom}*	*After LS (#4)*	*Change in power after LS*	
A (11)	PERC mono	**540**	536.71	-0.61%	535.28	-0.20%	-0.39%
B (11)	PERC bifi shingl.	**660**	636.76	-3.52%	636.09	0.16%	-0.11%
C1 (4)	TOPCon mono	**560**	551.47	-1.52%	550.05	-0.26%	-0.43%
C2 (10)	TOPCon bifi	**560**	547.63	-2.21%	547.69	-0.01%	-0.40%
D (12)	HJT mono	**375**	364.92	-2.69%	365.97	0.05%	-0.15%
E1 (13)	PERC mono	**655**	653.91	-0.17%	653.07	-0.09%	-0.32%
E2 (4)	TOPCon bifi	**560**	548.05	-2.13%	547.60	-0.08%	-0.35%

On average, the manufacturers have a measured power output **deviation** that is almost **-2%** lower than the nominal values and power tolerances of 0% to +3%. The maximum deviation is -3.52%. The values are at the limit or below the estimated measurement uncertainty of SUPSI PVLab (uP_m = ±1.9% [k=2;95%]) for measurements without spectral mismatch correction.

The power **degradation** observed after the **initial light soaking** of 10 kWh/m² is limited and, on average, does not exceed **−0.4%**.

The measured bifaciality values are consistent with those declared in the corresponding manufacturer datasheets. The indoor measurements of bifacial modules at SUPSI PVLab are conducted according to the single-source test method described in the International Electrotechnical Commission (IEC) Technical Specification IEC TS 60904-1-2.

The relative efficiency change with irradiance for each technology is shown in Figure 19. The modules with shingled cells (Tech #2) and HJT cell technology (Tech #5) show the lowest and highest loss at low irradiance, respectively. Since photovoltaic systems operate a large fraction of time with irradiance levels below STC conditions (e.g., during mornings, evenings, cloudy conditions, and winter periods), the low-irradiance behaviour of modules can have a measurable impact on the annual energy yield of the PV system. The electrical performance under low-irradiance conditions provides important information on the quality of the solar cells and module interconnections.

In the case of shingled modules, it should be considered that the shingling process typically involves cell cutting and adhesive interconnections, which may affect the electrical characteristics of the module by increasing series resistance or reducing shunt resistance. The better low-irradiance performance may be here related to the robust manufacturing process and cell quality, as well as the reduced inactive area associated with the shingled architecture.

Generally, HJT modules exhibit a high efficiency under standard test conditions and higher ambient temperatures; however, at low irradiance, the relative efficiency can be adversely affected by parasitic losses. The higher efficiency reduction observed in the here tested HJT modules may be related to the passivation layer, interface quality between a-Si:H and c-Si, or to the multi-wire interconnection, which, depending on the manufacturing process, can all potentially increase resistive and/or recombination-related losses under low irradiance.

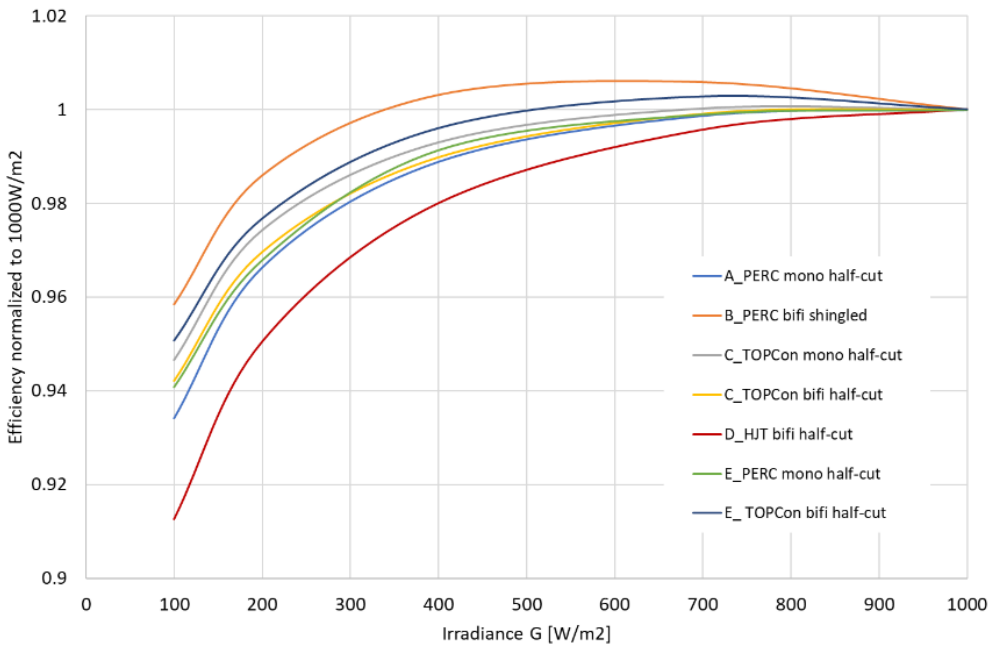

Figure 19: *Initial relative efficiency curves for all seven technologies and varying irradiance levels.*

Degradation analysis of field exposed modules

The degradation was evaluated on two occasions: first in September 2023 on the four dismantled modules after 10 months of outdoor exposure, and again in October 2024 on the reference modules after 13 months of outdoor exposure. Consequently, two independent datasets representing approximately the first year of outdoor exposure are available for analysis.

Table 7 presents the average power degradation (of 4 modules) measured in 2023 and 2024 for each module technology, together with the corresponding warranty declarations provided in the manufacturers' datasheets. The changes in EL images after field exposure are reported in the Annex.

Table 7: *Average absolute [%] and annual power degradation rates [%/y] of four modules for all 7 technologies measured for the replaced modules (repl) and the reference modules (ref).* *Note: Isc, Voc and FF degradation as well as single module measurement results are reported in the Annex Table.*

Brand	Type	Power warranty		$\Delta P_{m,repl}$ * [%]	$\Delta P_{m,repl}$ * [%/y]	$\Delta P_{m,ref}$ [%]	$\Delta P_{m,ref}$ [%/y]
		1st year	*after 1st year*	*after 10 months (01.12.2022-27.09.2023)*		*after 13 months (29.09.2023-22.10.2024)*	
A	PERC mono	-1%	-0.4%	-0.71%	-0.86%	-1.11%	-1.04%
B	PERC bifi shingl.	-2%	-0.45%	-0.94%	-1.15%	-1.53%	-1.44%
C1	TOPCon mono	-1%	-0.4%	-0.36%	-0.44%	-0.59%	-0.56%
C2	TOPCon bifi	-1%	-0.45%	-0.64%	-0.78%	-0.93%	-0.87%
D	HJT mono	-1%	-0.2%	-2.22%	-2.70%	-4.07%	-3.82%
E1	PERC mono	-2%	-0.55%	-1.52%	-1.85%	-1.62%	-1.52%
E2	TOPCon bifi	-1%	-0.4%	-0.30%	-0.36%	-0.67%	-0.63%

** in absence of the initial measurements the degradation rate is here calculated with respect to the average stabilised power of the screening tests shown in Table 6.*

Following technology-related conclusions could be drawn from the first year's measurements:

- **TOPCon and PERC modules** show degradation rates within the first-year warranty limits, with measured values ranging from **–0.3% to –1.62%**.
- **HJT modules** are the only technology exhibiting significant degradation in Pmax, Isc, and Voc (see also Annex). The degradation in Pmax reached up to **–4.07%**.
- **No evidence of PID was observed during the first two years of operation.** No significant differences were detected among the four modules distributed along the high-voltage strings (see Annex); suggesting the absence of PID degradation.

Only extended monitoring will determine whether the observed degradation trends stabilise or continue and if they align with the manufacturer-declared rates of –0.2 to –0.55 %/year.

The notably higher degradation of the HJT modules is here analysed in more detail.

Performance loss in HJT

Previous studies cited in the recent IEA PVPS Task 13 report [17] highlights that heterojunction cells are sensitive to stressors such as moisture, heat, and irradiance. These stresses contribute to degradation mechanisms, including light- and temperature-induced degradation as well as UV-related effects and material degradation in modules. The severity of these degradation mechanisms depends

on the materials used and module design and therefore may vary between manufacturers. The problem is generally mitigated by appropriate BOM and module manufacturing.

Furthermore, in a previous SFOE project (ATTRACT SI/502036-01) conducted by SUPSI PVLab on commercial glass/backsheet HJT modules, a strong degradation in Pmax in the range of -5.75%/year in the first year and -1.57%/year in the second year was observed due to a poor bill of material, which did not prevent the penetration of the humidity through the backsheet, and a minor degradation was observed in Isc and Voc of -2.3%/year and -1.35%/year, respectively. The Isc and Voc losses seemed to stabilize over time. The reduction of Voc is a typical consequence of UV-induced degradation mechanisms which are caused by the deterioration of the UV-exposed front passivating layers.

As expected for glass/glass modules, the modules in Viganello are less prone to humidity-induced degradation mechanisms, as confirmed by the reduced presence of humidity related defects in the electroluminescence images (see EL pictures in Annex), but similar Isc and Voc degradation behaviours as in the glass/backsheet modules were observed.

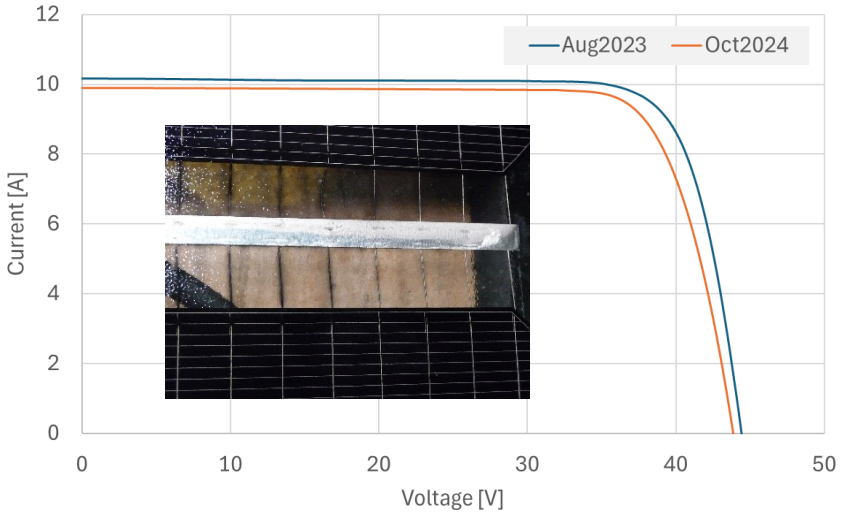

Figure 20: *I-V curves measured before and after 13 months of outdoor exposure together with a detail of cell-interconnection degradation.*

In addition, some yellowing of the encapsulant at the cell inter-connects and darkening of the contact fingers are observed (see Figure 20). The reduction in short-circuit current and fill factor, together with minimal change in Voc in the I–V curve after 13 months of field exposure, indicates an increase in series resistance, likely caused by degradation of the cell interconnections.

Figure 21 shows an initial delamination of the contact fingers at the border cells observed on outdoor exposed modules. This failure is already known by the manufacturer and reported as an aesthetic issue, which shouldn't affect performance. The condition will nevertheless be monitored over time.

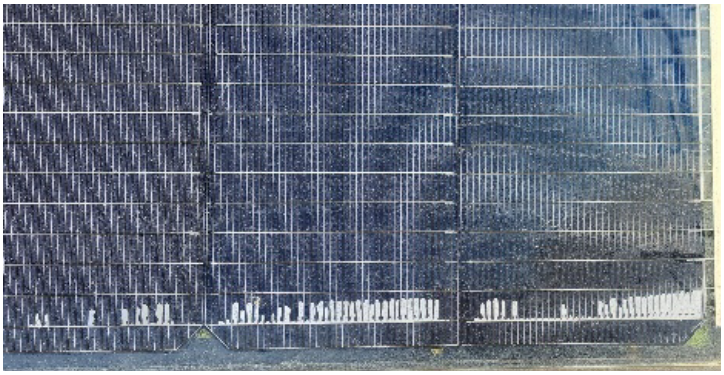

Figure 21: *Tech #5 (HJT) modules: delamination of the contact fingers.*

3.4.2 Field inspections

Visual inspections conducted on all modules as part of the project identified additional failures, which are discussed in the following.

Glass breakage

Between June 2023 and December 2025, three PV modules exhibited glass breakage at the Viganello site. All affected modules belong to Technology #2 (PERC bifacial shingled) modules installed on the North tower in string 3. Their positions are indicated in Figure 4. Notably, one of the failures occurred after the replacement of a previously broken module.

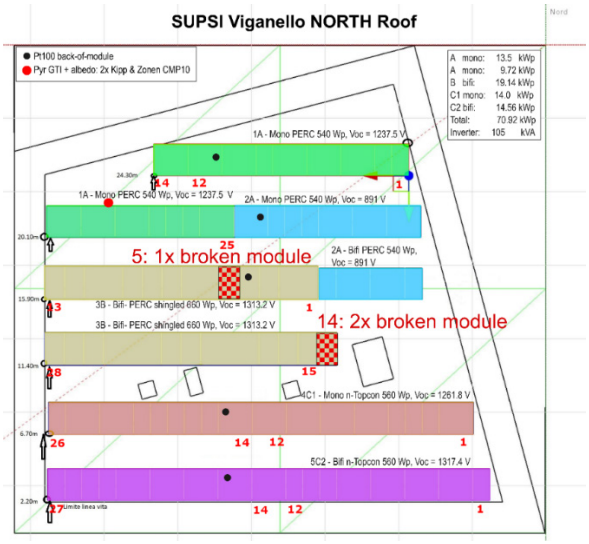

Figure 22: *Viganello North Tower, with location of broken shingled modules marked.*

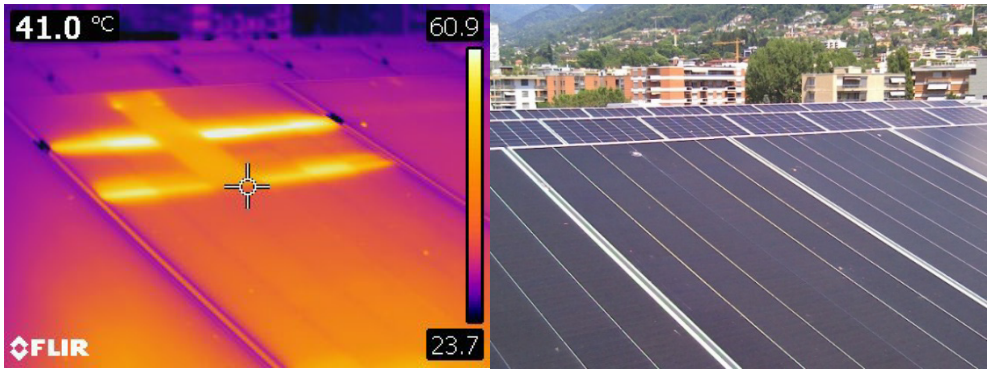

Figure 23: *IR image of the broken module (left) Broken module photo (right) (Tech #2)*

Of the broken modules observed in 2023, one module had an object impact point with probable fusion causing the front and back glass to break. The string continued to function, although the module suffered a -16% power decrease, caused by a 3 A current decrease on one part of the module with the consequent activation of the by-pass diode (see Figure 23). The second broken module showed glass damage with a -6.5% power decrease *without* a bypass diode activation.

The affected modules consist of glass–glass laminates with 2 mm front and 2 mm rear glass. Although the manufacturer datasheet specifies tempered front glass, literature indicates that glass below 2.8-3.2 mm thickness is typically heat-strengthened rather than fully tempered [18], which is consistent with the observed fracture patterns (Figure 25) and in contrast with theory (*Figure 24*).

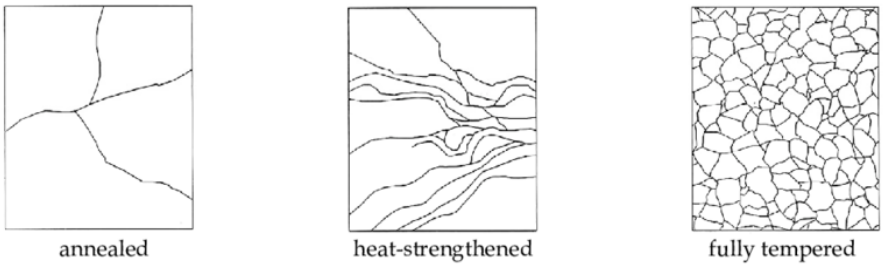

Figure 24: Fracture pattern of annealed, heat strengthened and fully tempered glasses.

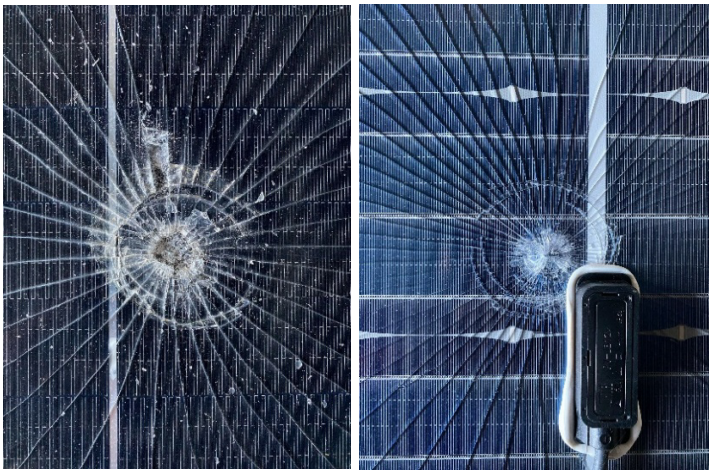

Figure 25: *Front (left) and rear (right) side of the impact on the module in position #5, Tech #2.*

Detailed investigations of modules #5 and #14 indicate that blunt object impacts were the primary cause of glass breakage. Site inspections revealed the presence of soft and hard foreign materials (e.g., moss, stones, metal fragments) on module surfaces, likely dropped by birds, supporting the impact-based root-cause hypothesis. Module #5 experienced a single high-stress impact, evidenced by radial and concentric fractures (Figure 25) followed by electrical disconnection (Figure 27), and secondary thermal stress fractures in both front and rear glass (Figure 28). Additional fractures parallel to the module edges likely developed after the impact due to self-weight stress acting on the thin glass. The absence of ultraviolet fluorescence (UVf) at the impact point, except at the detected secondary thermal stress fracture point, indicates that the area did not experience elevated temperatures before or after the crack occurred (Figure 26). Module #14 exhibited two lower-stress impact points, indicated by radial fractures without concentric cracking and no detectable electrical or thermal anomalies in EL or UVf images (Figure 29).

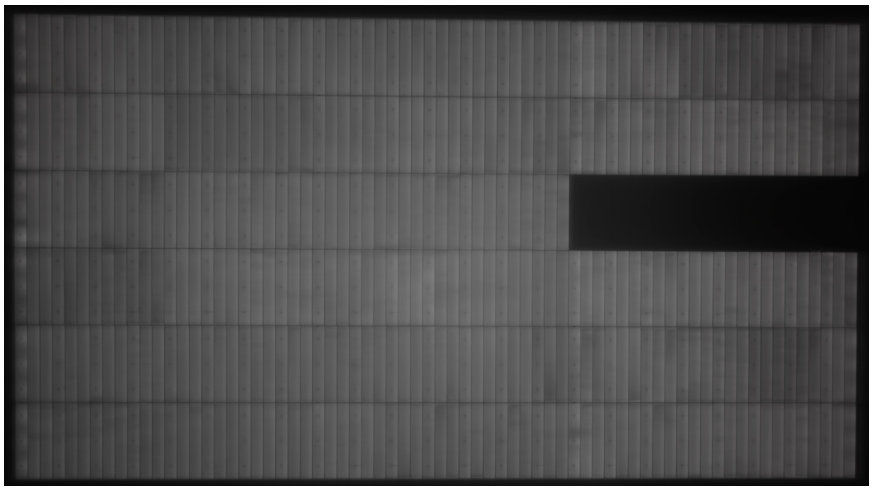

Figure 26: *EL image of the module in position #5.*

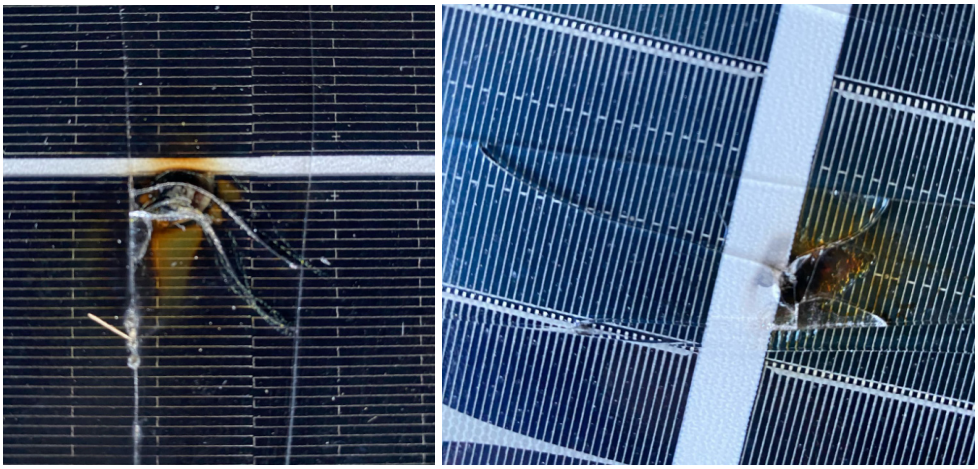

Figure 27*: Close-up images on the thermally stressed areas and thermal fractures (wave-shape) of (left) front and (right) rear sides of the module in position #5.*

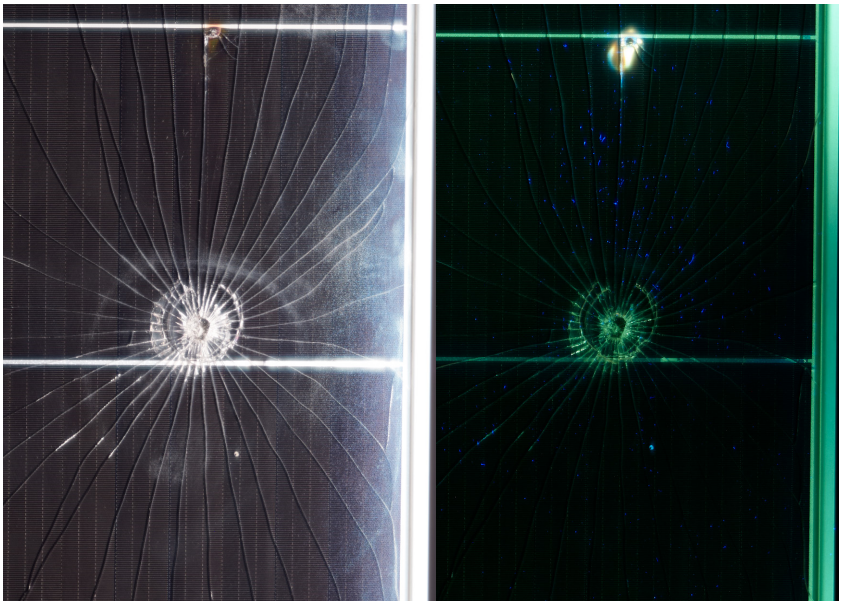

Figure 28: *Close-up (left) visual inspection and (right) UVf images of the module in position #5.*

Figure 29: *Front side of the impact on the module #14.*

While the site visits and visual inspections have shown their value in detecting glass breakages, these failures do not appear to be easily detectable in the electrical performance data alone.

The repeated module breakage in 2025 in the same position #14 is not clearly visible to the naked eye, unless special attention to this phenomenon is applied, see Figure 29. It is not clear whether this breakage is due to local shading effects, or again due to blunt object impact. The breakage pattern is less obvious than those found in the first two broken modules.

Figure 30: *Whole-of-module view of broken module #14 (second module breakage in this position, left), and detailed view on glass crack (right).*

The consequence of visual inspection not detecting glass breakage easily (on top the difficulty and cost of scaling this to larger power plants) is that this requires other detection techniques (EL, UVf, …) that also need to be applied regularly. If true, this would put a floor to O&M costs, meaning that future O&M costs may not continue to decline (as fast) over time.

<u>System failure: Series fuse failures</u>
Two series fuse failure events were recorded. Despite there being no parallel strings of modules connected to one MPP tracker, two string fuses were added, one on the positive side and one on the negative side, due to the presence of the data acquisition system, and especially the dark I-V system.

The two fuse failure events caused prolonged outages in the same string (Tech #6, String 4E1 on the South Tower) between 23 March 2024 and 15 June 2024. This long repair time was due to the difficulty in obtaining 1500 Vdc fuses with the necessary characteristics: capable of operating at 1500 Vdc, having a continuous current rating of 25 A or 30 A, and the necessary reaction speed. Unfortunately, it was not possible to determine the cause of the problem with certainty.

- One possible hypothesis is the high short-circuit and maximum power current of the modules ($I_{sc,STC}$ 18.43 A, $I_{mp,STC}$ 17.36 A), which can be further amplified by over-irradiance events. At Viganello, irradiance values exceeding 1400 W/m² and even 1500 W/m² (1-minute values) are routinely measured, with peak clear-sky values at noon around 1100 W/m² (i.e. irradiance continuously for an hour or longer, more than 10% above STC conditions). In the case of 1400 – 1500 W/m^2, the MPP current can reach 26 A. Data from the literature [19] has over-irradiance events often being of shorter duration (5-60 seconds), where higher values of 1600 – 1700 W/m² are observed for such bursts, yet occasionally lasting up to 1-2 minutes. As the irradiance and power data is measured at 1-minute resolution, it is not possible to identify whether short-term over-irradiance effects caused the fuse strings to operate.

- An alternative hypothesis may lie with the production quality of the fuses: after discovering the fuse issue, 1500 Vdc fuses were purchased, some of which were measured prior to installation to have a very high series resistance R_S. As the power dissipation within the fuse during normal operation is related to $P_{dissipation} = R_S * I_{mp}^2$, and therefore the fuse R_S may have resulted in the fuse operating (i.e. melting) due to high continued current passing through.

System failures: Soiling, row-to-row shading and hotspots

While not as easily visible on whole-of-module photographs, inhomogeneous soiling was present over most modules and arrays, both on the North and South towers. This inhomogeneous soiling resulted in local hotspots (Figure 30 and Figure 31). As the peak plane-of-the-array irradiance in December is ~600 W/m² to 700 W/m², while ambient temperatures are low, this inhomogeneous soiling does not (yet) result in high absolute temperatures of the hotspots, with peak temperatures reaching 25°C to 30°C. It is expected that the soiling-induced hotspots will reach higher temperatures in the summer months, although the magnitude is not known at this time.

Of note, the soiling sensors do not seem to capture this inhomogeneity of soiling well, which may also be due to the smaller size of the soiling sensors, compared to the PV modules.

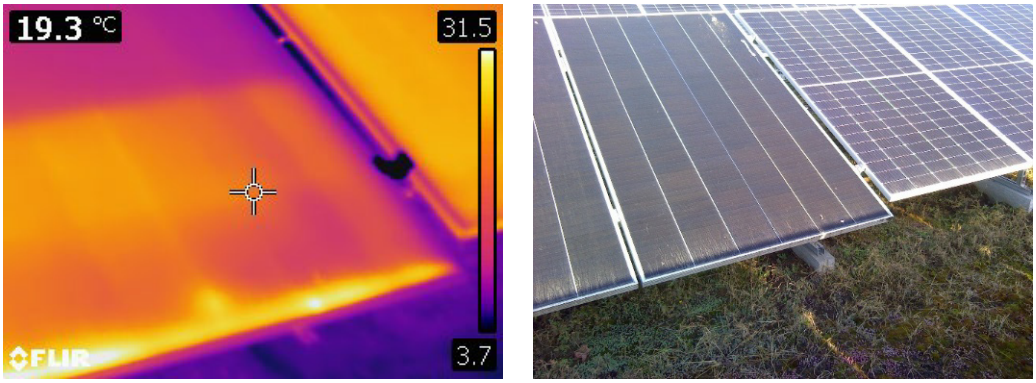

***Figure 31**: Detail of row-to-row shading on String 3B-Tech #2 (North tower), and thermal impact, measured on 12 December 2025. Row 2A-Tech #1 next to it is shade-free, as the bottom of the module is higher off the ground. Both strings have inhomogeneous soiling, which is concentrated at the bottom of the module.*

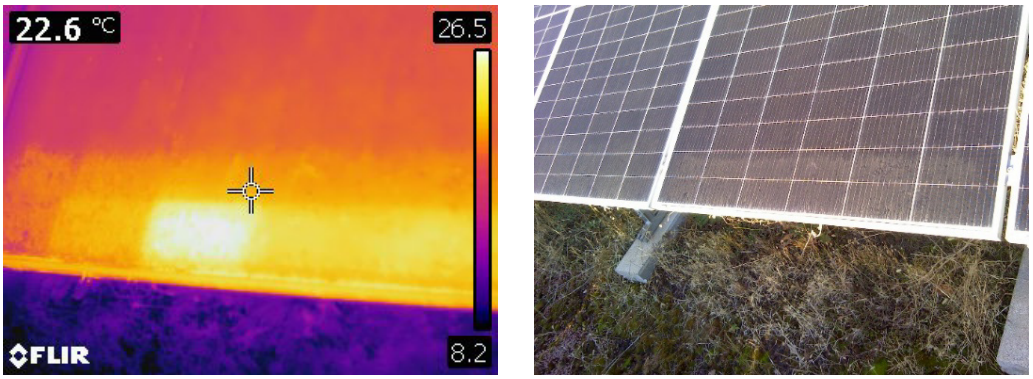

***Figure 32:** Local hotspot(s) due to inhomogeneous soiling, Tech #6, String 4E1, South Tower.*

3.5 System monitoring data analysis

3.5.1 Data processing and calculations

Although the system in Viganello was installed in December 2022, it was not commissioned until June 2023 due to various legal issues between the Distribution System Operator (DSO) and USI/SUPSI. The plant was commissioned in June 2023 and the data acquisition system started in the same month.

Typical contracts for PV EPC (Engineering, Procurement and Construction) companies have a 2-year defects period, where any performance or workmanship errors have to be remediated. This may include data (monitoring) issues, sensor replacements, and even module replacements if needed. Continuous performance monitoring is therefore important during the early operational phase of a PV system.

Compared to laboratory measurements, outdoor monitoring data analysis may require more steps to calculate valid key performance indicators (KPIs), especially to achieve fair comparisons. Figure 32 shows the general process that must be undertaken to go from raw data to the final KPI.

Figure 33: *High-level process from measurement to KPI calculation*

While many key performance indicators (KPIs) can be used to evaluate the PV system performance [20], the dominant KPI to determine performance and quality of PV systems remains the Performance Ratio (PR), often also used in its temperature-corrected form. Table 8 gives the KPIs and their definitions that will be discussed further in this chapter. The benefit of using the temperature-corrected form of PR and η_N is that this corrects for well-known temperature impacts on system efficiency and yield, which allows comparisons between technologies as well as across different times of the year. These temperature-corrected KPIs thus have a better signal-to-noise ratio, providing clearer insights into the relative performance of system.

Table 8*: Key Performance Indicators (KPIs) and their definitions.*

	Regular form	Temperature-corrected form
Performance Ratio	$PR = \frac{E_{PV}/P_{STC}}{H_{POA}/G_{STC}}\ [\%]$	$PR_{tc} = \frac{E_{PV,tc}/P_{STC}}{H_{POA}/G_{STC}}\ [\%]$ With $E_{PV,tc} = \sum \frac{\overbrace{P}^{P_{PV,tc}}}{1+\gamma*(T-T_{STC})} * \Delta t$
Normalised efficiency	$\eta_N = \frac{P_{PV}/P_{STC}}{G_{POA}/G_{STC}}\ [\%]$	$\eta_{N,tc} = \frac{P_{PV,tc}/P_{STC}}{G_{POA}/G_{STC}}\ [\%]$

Whereas the previous chapters described how data are measured, this chapter will focus on the 3 consecutive steps: data quality control and correction, calculation of derived data, data filtering and KPI calculation.

Data quality control and corrections

Considering the purpose of the RACONT2050 project is to gain insights into module technologies, corrections need to be made for an as-fair-as-possible comparison.

The main applied corrections are listed below:

- The string 4E1 was down for ~3 months (23 March to 15 June 2024) due to a broken fuse; this data was replaced using a linear regression model using strings 3D and 5E2 (mean absolute error for the period 16 June to 31 August 2024: 0.6%).
- Some temperature sensors had a slight air gap which results in higher nighttime temperatures, and slightly lower daytime temperatures. For missing data and clearly erroneous data, temperature sensor data was replaced with data from surrounding strings with similar thermal behaviour, by determining linear regression coefficients during moments of correct operation. The benefit of having multiple temperature sensors available allows for data redundancy, as well as allowing sensors to be compared to the mean of each roof.
- When at least one string was not operational, e.g. for reference module measurements or site maintenance, all data for that period (hours or days) was discarded for Performance Ratio calculations. For example, the 28 reference modules were temporarily removed for indoor laboratory measurements from 27-29.09.2023 and 22.10-7.11.2024, during which the corresponding strings were offline.

Calculation of derived data: reference irradiance for bifacial modules

Some physical parameters required for the calculation of the KPIs, are not measured directly by the monitoring system and therefore must be derived from the available measurements. One example is the effective irradiance for bifacial modules, which accounts for the contribution of rear-side irradiance and depends on the bifaciality of the module technology.

Not all of the rear irradiance contribution for bifacial modules is considered at the same level as the front side, due to each module's bifaciality value. The bifaciality factor of every cell/module technology is different. The bifaciality of the 4 different technologies in Viganello varies between 70% to 90% (see Table 6).

To calculate the effective rear irradiance (for a particular module technology), the measured rear irradiance is multiplied with bifaciality:

$$G_{Total} = G_{POA} + [(G_{RPOA}) \times (bifaciality)]$$

Where:
G_{Total}: total bifacial irradiance;
G_{POA}: front side plane-of-array measured irradiance;
G_{RPOA}: measured rear plane-of-array irradiance.

The last is influenced by the albedo (the ratio of the ground-reflected to the global-horizontal irradiance), as well as how high off the ground modules are. Modules closer to the ground (such as at Trevano) have much lower potential for G_{RPOA} than at Viganello. Conversely, gravel reflects sunlight better than a green roof. If the Viganello roof would be covered with gravel instead, the same systems are expected to have a slightly higher bifacial yield.

For bifacial modules, G_{total} replaces G_{poa} in the equations for PR and η_N from Table 8, which then allows monofacial and bifacial modules to be compared with these metrics.

The in-plane albedo measurements of RACONT installations in Campus Viganello and Campus Trevano are measured by albedometers, see Figure 33. At each site, two pyranometers are installed: One pyranometer is installed in the plane of the array to measure the global plane-of-array irradiance (G_{POA}), while the second one is placed in the rear plane of the array, to determine the global reflected irradiance (G_{RPOA}).

Figure 34: *Placement of the G_{POA} and G_{RPOA} sensors at Viganello (left) and Trevano (right).*

Data filtering: shading

To ensure a fair comparison between technologies, all systems should ideally operate at their best possible condition. However, the arrays are subject to unequal amounts of shading throughout the day and the year. This therefore requires for shading to be first detected, to then exclude the moments when arrays are shaded. Figure 34 shows that most intense shading is experienced in the mornings, with some systems also experiencing afternoon shading. To the east of Viganello the mountain Monte Brè (925 m) causes far shading in the morning on both roofs. Additionally, shading occurs throughout the year from surrounding buildings at intermediate distances (10–500 m), such as the USI/SUPSI buildings located east of the South tower and west of the North tower (see Figure 2), as well as from nearby obstacles (<10 m), e.g. row-to-row shading, and shading from technical bodies on the roofs.

The PV strings on the North and South towers experience different amounts of near and far shading. To ensure fair comparisons, the following data filters and, where necessary, data corrections were applied:

- All strings had to be operational at the same time, with validated or corrected data available;
- Temperature-corrected normalised efficiencies had to be within a 10%-point spread of the mean per roof: if one system deviated from this (e.g. due to shading), then all data is discarded for that point in time.

The practical consequences of these strict filtering criteria is that much of December is excluded, as System 3B (North) experiences continuous row-to-row shading between ~7 December and 31 December.

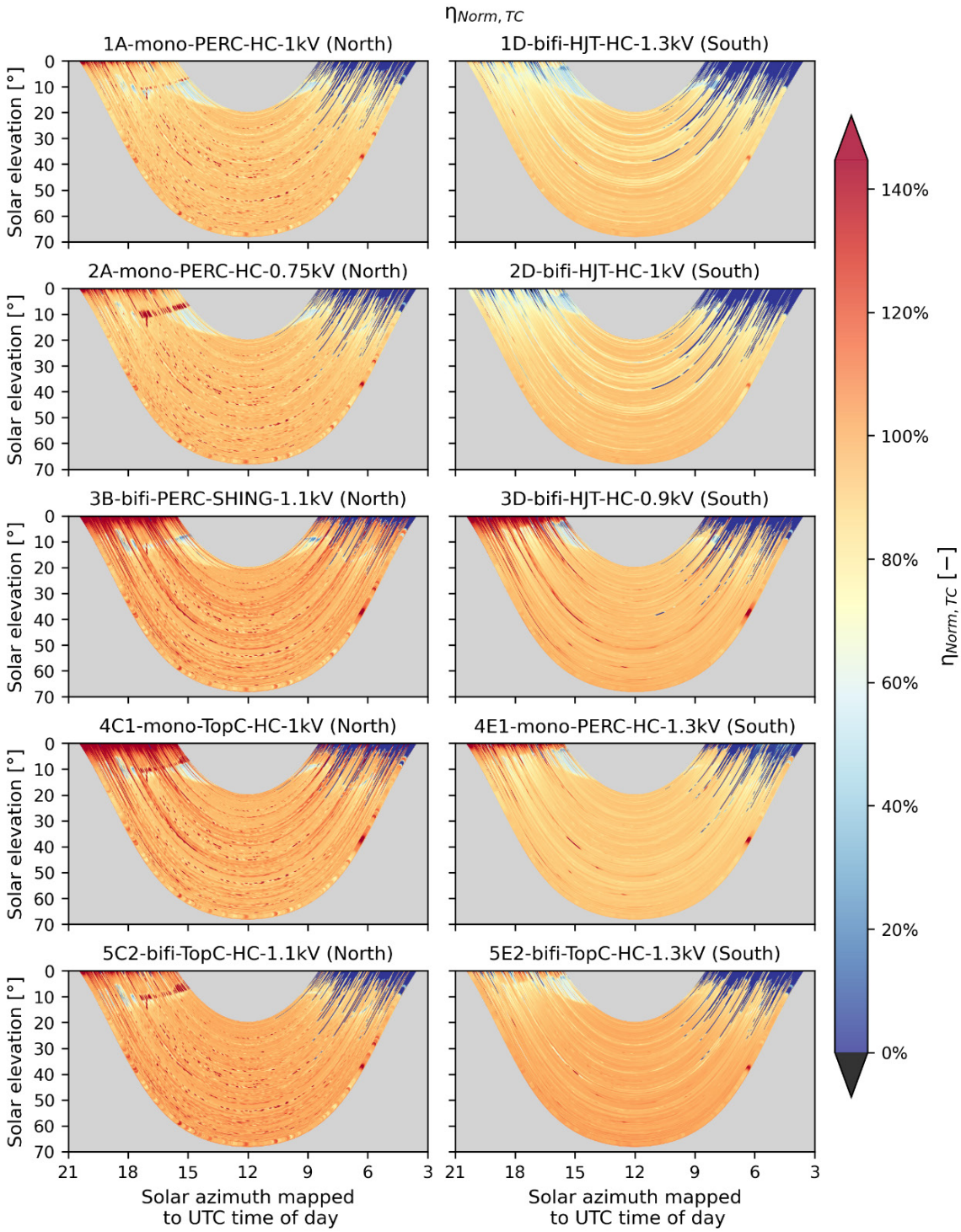

Figure 35: *Temperature-corrected normalised efficiency diagrams for the respective strings at Viganello, shown throughout one year. Dark blue areas show that a string suffers more shading than the average of the strings at that time, dark red shows over-performing strings (e.g. one string with less shading than others). Light blue (e.g. string 1D-bifi on South tower around 15h) indicates row-to-row shading losses in winter months.*

3.5.2 Performance Ratio analysis

Impact of shading on PR and PRtc

Figure 35 and Figure 36 allow comparison of the impact of shading and temperature on the monthly performance ratio. Figure 35 gives insights into how much shading affects the yield, especially in the winter months. By contrast, Figure 36 allows for a better comparison between technologies, as most of the temperature and shading effects have been filtered out.

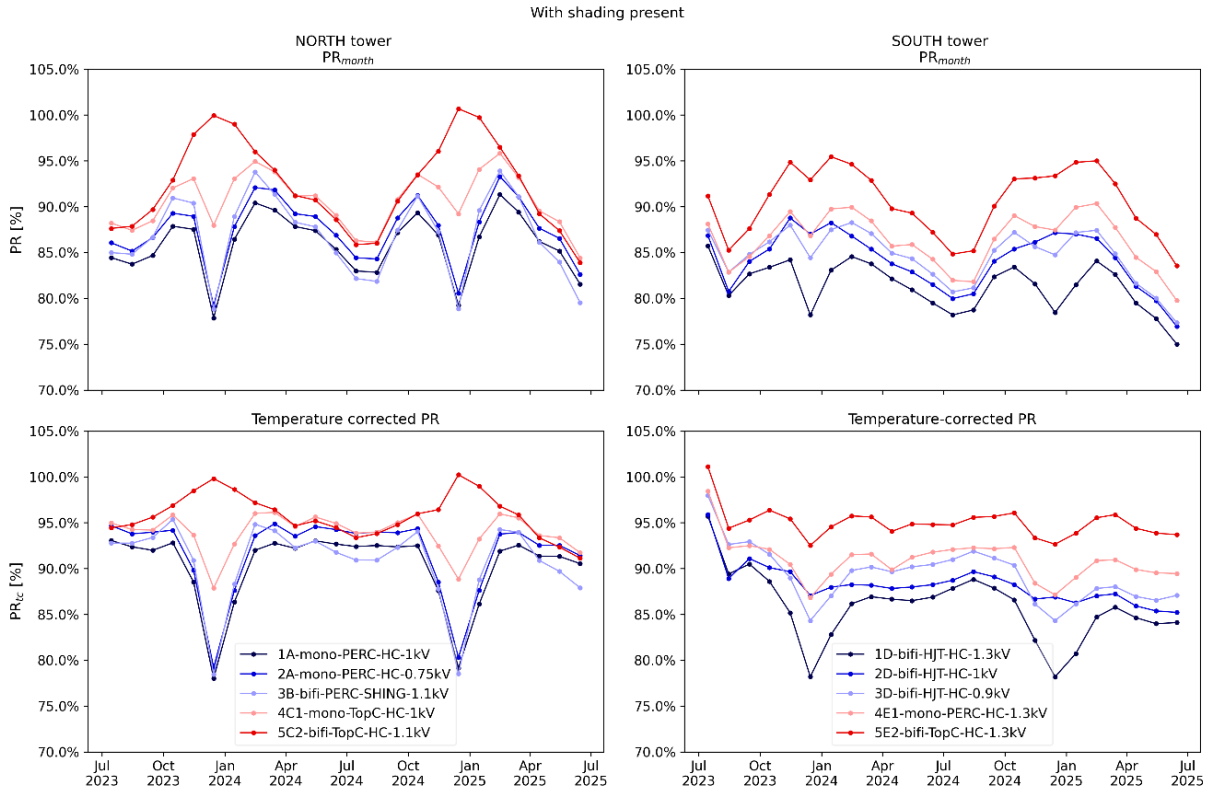

Figure 36: *Shaded monthly PR and temperature-corrected PRtc for the different strings and technologies.*

In Figure 36, both systems 5C2 and 5E2 appear to be performing significantly better than the others, especially 5E2 (South tower). This performance is positively impacted by their relative position (see also Figure 2 and Figure 4). Both strings are the Southern-most on the respective roof, and hence:

- Suffer very little nearby shading, and have no row-to-row shading;
- Benefit most from their bifaciality: there is an almost obstacle-free near horizon, whereby the most sunlight can be captured by their rear surface, and this light can also pass unimpeded from the front of the module. In winter the lower position of the sun also provides the largest benefit to the front row, while the other rows see less of the illuminated sky due to row-to-row obstructions.
- System 5E2 (S) also has the least obstacles that can impede irradiance to reach it, while system 5C2 (N) has two USI buildings (East and South) that also block some diffuse irradiance.

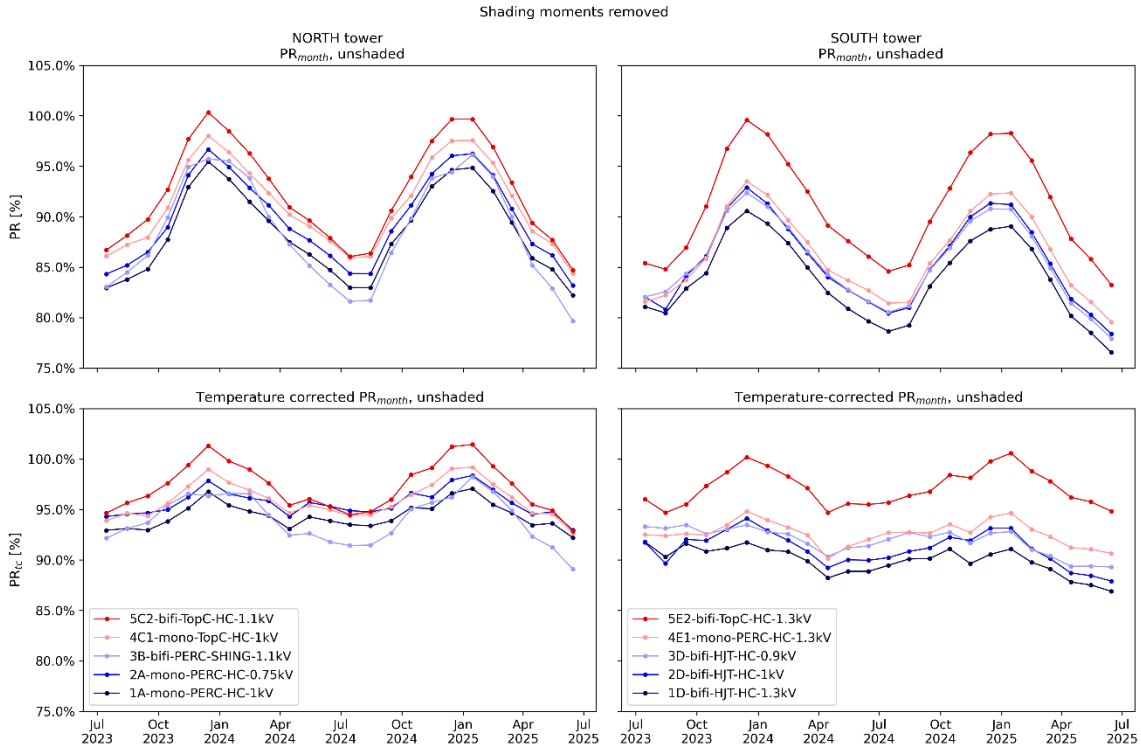

Figure 37: *Unshaded monthly PR and PRtc for the different strings and technologies.*

3.5.3 Technology inter-comparison

In general, the TOPCon strings have a 3.1%-point energy yield advantage compared to PERC, which itself is 3.1% points higher than HJT, as seen in the Performance Ratio (Table 9 and Table 11). The yield advantage of TOPCon reduces slightly when correcting to STC temperature conditions (Table 10 and Table 12), yet bifacial TOPCon still has a 1%-point PRtc advantage over monofacial TOPCon.

Table 9: *Two-year average unshaded Performance Ratio by technology at Viganello.*

	TOPCon	**PERC**	**HJT**
Monofacial	89.1%	86.0%	
Bifacial	89.1%	86.0%	82.9%
All	**89.1%**	**86.0%**	**82.9%**
Difference to TOPCon		**-3.1%**	**-6.2%**

Table 10: *Two-year average unshaded temperature-corrected Performance Ratio by technology at Viganello.*

	TOPCon	**PERC**	**HJT**
Monofacial	95.1%	93.7%	
Bifacial	96.2%	93.1%	90.7%
All	**95.9%**	**93.6%**	**90.7%**
Difference to TOPCon		**-2.3%**	**-5.1%**

Table 11: *Unshaded Performance Ratio data for the RACONT systems at Viganello.*

PR NORTH Tower	**1A mono PERC** HC 1 kV	**2A mono PERC** HC 0.75 kV	**3B bifi PERC** SHING 1.1 kV	**4C1 mono TopCon** HC 1 kV	**5C2 bifi TopCon** HC 1.1 kV
Year 1	86.5%	87.9%	86.9%	89.5%	90.6%
Year 2	85.9%	87.3%	85.1%	88.7%	89.3%
Average	**86.2%**	**87.6%**	**86.0%**	**89.1%**	**89.9%**
PR SOUTH Tower	**1D bifi HJT** HC 1.3 kV	**2D bifi HJT** HC 1 kV	**3D bifi HJT** HC 0.9 kV	**4E1 mono PERC** HC 1.3 kV	**5E2 bifi TopCon** HC 1.3 kV
Year 1	82.7%	84.0%	84.4%	84.6%	88.6%
Year 2	81.0%	82.8%	82.6%	83.8%	87.9%
Average	**81.9%**	**83.4%**	**83.5%**	**84.2%**	**88.3%**

Table 12: *Unshaded temperature-corrected Performance Ratio data for the RACONT systems at Viganello.*

PRtc NORTH Tower	**1A mono PERC** HC 1 kV	**2A mono PERC** HC 0.75 kV	**3B bifi PERC** SHING 1.1 kV	**4C1 mono TopCon** HC 1 kV	**5C2 bifi TopCon** HC 1.1 kV
Year 1	93.7%	95.1%	93.5%	95.2%	96.4%
Year 2	93.9%	95.1%	92.6%	95.1%	95.8%
Average	**93.8%**	**95.1%**	**93.1%**	**95.1%**	**96.1%**
PRtc SOUTH Tower	**1D bifi HJT** HC 1.3 kV	**2D bifi HJT** HC 1 kV	**3D bifi HJT** HC 0.9 kV	**4E1 mono PERC** HC 1.3 kV	**5E2 bifi TopCon** HC 1.3 kV
Year 1	90.2%	90.9%	92.3%	92.2%	96.0%
Year 2	89.3%	90.3%	91.4%	92.4%	96.6%
Average	**89.8%**	**90.6%**	**91.9%**	**92.3%**	**96.3%**

The results above indicate that there are also meaningful differences to be seen between manufacturers, and that a headline technology (PERC, HJT, or TOPCon) does not tell the full story about likely performance in the field. For example, the modules from manufacturer C (4C1 and 5C2) appear to have a 1.5%-point reduction in thermal losses compared to the other systems, see Figure 37.

Nevertheless, out of the seven technologies tested at Viganello, five achieve a high DC-measured Performance Ratio. These results show the significant improvements to the performance ratio that the PV industry has achieved over time [21].

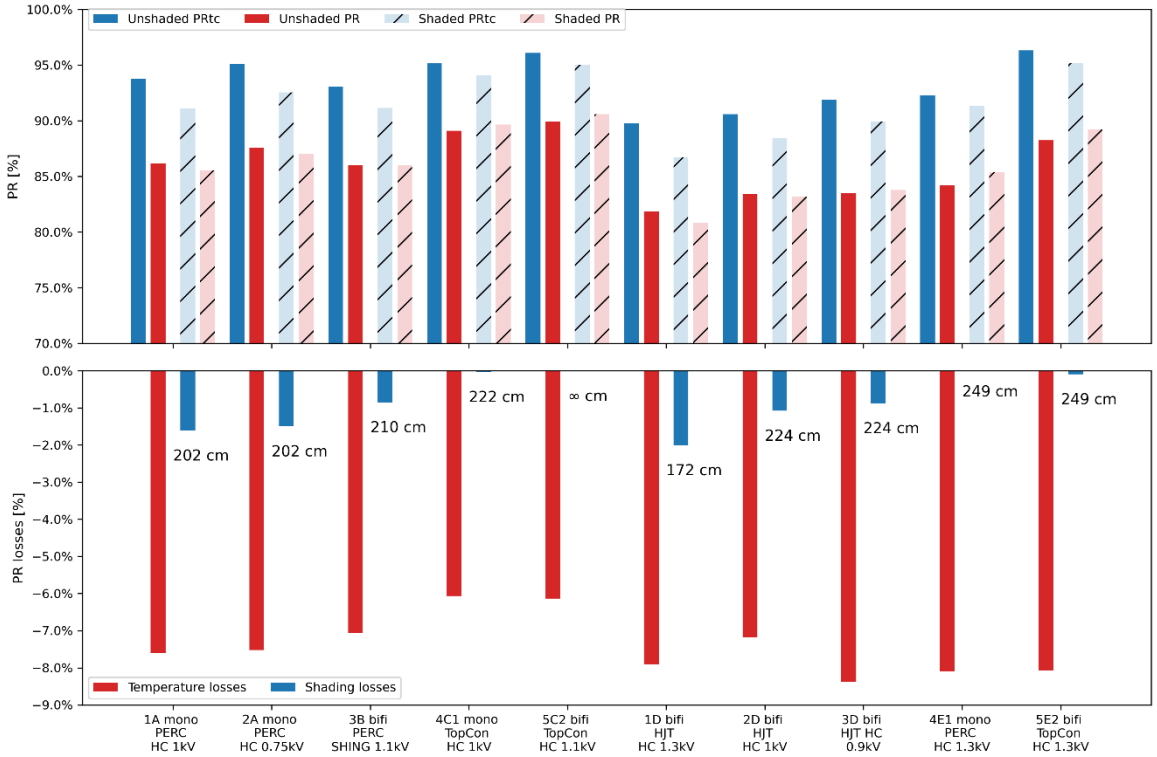

Figure 38: *Average PR and PRtc, (shaded and unshaded), calculated over two years of operation. The difference between PRtc and PR indicates the average temperature losses per string, technology, and manufacturer. Shading losses are also shown, with the row-to-row distance that the string experiences (see Figure 4).*

The shading losses in Figure 37 also vary by technology, as well as the row-to-row shading that each string experiences. Additional shading losses are from the surrounding buildings, as previously discussed. The shading losses' impact on the annual PR and PRtc are generally limited in magnitude, as these shading losses primarily occur during low-irradiance moments (mornings, evenings, and in winter).

3.5.4 Bifacial gain

Figure 38 shows the bifacial yield gain of the bifacial modules, which is calculated as:

$$PR\ bifacial\ gain = PR_{bifi} - PR_{mono}$$

The PR for the bifacial modules is thus also calculated as if these were monofacial (therefore using only G_{POA} as the reference irradiance). This answers the question "how much more do bifacial modules produce than their monofacial equivalent?". As expected, given the analyses above, the modules on the front row of each flat roof have a larger bifacial benefit (0.2%-points to 0.6%-points) versus the other strings. The seasonality of the bifacial gain is clearly visible, a consequence of the higher position of the sun in summer versus winter. Compared to values shown, bifacial modules installed high off the ground can achieve 5%-15% yield benefits [22], whereas modules installed next to the ground surface (i.e. the lowest part of the module touches the ground) achieve ~2% bifacial gain [23]. The annual bifacial gain observed for the Viganello systems at 3%-4% is at the lower end, in line with the expectations [24], due to the low installation height off the roof surface, and the measured albedo (average 4.8%). The

measured albedo is the *tilted* albedo, instead of the typical *horizontal* albedo. Nevertheless, an average albedo value of 4.8% is much lower than often used in the literature, e.g. 10% to 50% [24][25]. The seasonality in the measured albedo (and the bifacial gain) correlates to the maximum sun elevation throughout the year, with peak elevation at 70° in summer and only ~20° in winter (see Figure 34).

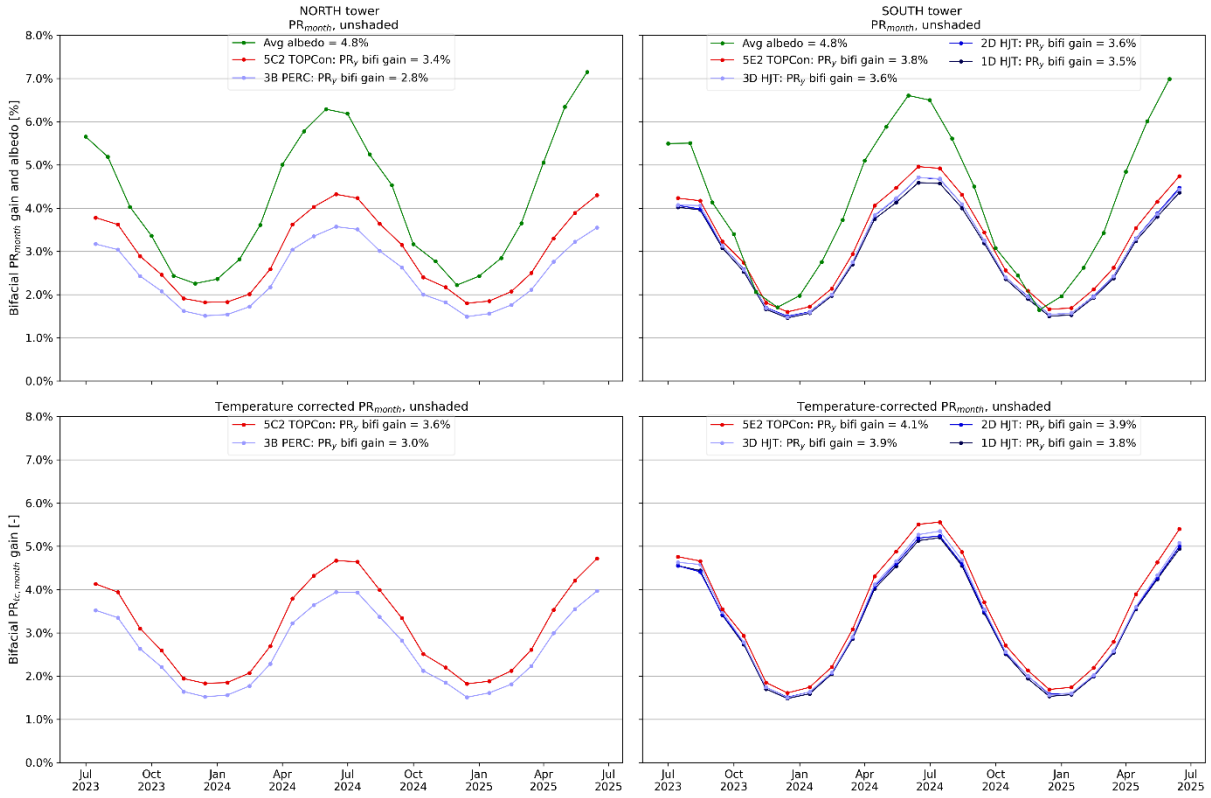

Figure 39: *Monthly unshaded Performance Ratio (regular and temperature-corrected) gain for bifacial modules, with the annual gain indicated in the legend. The measured albedo varies slightly for the two roofs, while the average is essentially identical.*

4 Summary & Conclusions

Below, the main achievements and key takeaways of the RACONT2050 project are listed.

- Successful deployment of a long-term, reference PV plant with high voltage strings: A 132.1 kW rooftop PV system was implemented at the USI/SUPSI Viganello campus, integrating seven state-of-the-art module technologies (PERC, TOPCon, HJT; mono- and bifacial) on 1500 V strings with dedicated monitoring. Despite spatial, shading, regulatory, and inverter constraints, the plant meets the project's objectives of accessibility, technological representativeness, and long-term data availability (>30 years).
- Robust experimental framework for technology comparison and degradation studies: The combination of high-voltage rooftop strings in Viganello and low-voltage reference strings in Trevano (including comparison with the historic 1982 TISO system) establishes a unique testbed to study performance, shading effects, bifacial behaviour, and potential-induced degradation (PID) across technologies under real operating conditions.
- Robust long-term data infrastructure and fair comparison methodology: The high-resolution (1-minute) monitoring system integrated into the Siemens domotic platform of the university campus ensures reliable operation and data continuity up to 2050. Rigorous data quality control, correction, and filtering procedures (including regression-based gap filling, sensor cross-validation, and strict exclusion criteria) were implemented to enable an as-fair-as-possible performance comparison between technologies under non-uniform shading and operational constraints.
- Development of a novel high-voltage dark I-V monitoring system: An innovative, low-cost Dark I-V Measurement System (DIVMS) capable of operating up to 1500 V and 20 A was successfully designed, simulated, and prototyped. The system overcomes limitations of existing commercial solutions by using a capacitor-based energy storage and linear regulation approach, enabling accurate, automated nighttime diagnostics of PV strings, independent of weather conditions.
- Proven diagnostic capability and integration into real PV plants: Laboratory tests on damaged modules and emulated string faults demonstrated that the DIVMS can reliably detect small changes in series and shunt resistance and other degradation indicators within large PV strings. The Viganello PV system was specifically designed to allow integration of the DIVMS and to enable automated nighttime I–V measurements. However, the automatic nighttime operation in Viganello still needs to be fully implemented.
- First reliability insights from visual inspections: Visual inspections of the Viganello system identified localized repeating module defects (glass breakage) in bifacial PERC shingled modules and early warning signs (contact finger failures) in HJT modules, while the PV strings largely remained operational. Two unexpected string fuse failures highlighted reliability challenges of operating at 1500 Vdc under high-irradiance conditions, emphasizing the importance of component selection and over-irradiance considerations in high-power rooftop systems.
- STC power underrating: Indoor characterisation showed that, on average, the measured STC power of modules is ~2% below nominal values, lying at the lower bound of manufacturers' stated power tolerances (0 to +3%). Initial light-induced degradation (LID) measured indoors were generally low (<0.4%). Bifaciality values are all consistent with datasheets.
- Insight into first year STC power degradation rates: Laboratory measurements confirmed that almost all technologies operated within the first-year warranty degradation limits, except for the

HJT modules which exhibited significantly higher early degradation, linked to cell-interconnection failures. No potential induced degradation (PID) in high voltage strings could be observed in the first two years.

- Consistent performance trends with site- and configuration-driven differences: After corrections, measured yields and performance ratios are good to very good, show good year-to-year consistency and broadly align with expectations. Bifacial strings in favourable positions (front rows) demonstrate clear performance advantages.
- High overall performance ratios across all systems: All systems have a good-very good Performance Ratio, with the AC-equivalent PR exceeding 80% (two systems) and 85% (five systems).
- Superior performance of TOPCon technology: Over the first two years of operation, the Performance Ratio of TOPCon exceeds that of PERC by about 3 percentage points and that of HJT by about 6 percentage points. Bifacial TOPCon achieves the highest temperature-corrected Performance Ratio and provides an additional benefit of about 1 percentage point compared with monofacial TOPCon. These results help explain the rapid transition of the PV industry from PERC to TOPCon.
- Measured bifacial gain and influencing factors: The annual bifacial gain ranges between 3% and 4%, with monthly variations correlating with albedo and solar elevation. Higher bifacial gains could be achieved with increased module elevation above the roof and with surfaces of higher albedo.
- Soiling and shading as drivers of local hotspots: Inhomogeneous soiling and shading increasingly lead to localized hotspot formation as time progresses, particularly where accumulated soiling is insufficiently removed by rainfall. A discrepancy between soiling sensor measurements and observed performance and reliability trends was also identified. Potential glass breakage related to local shading effects is currently under investigation.

5 Outlook

The benefits of the RACONT2050 project will grow over time, with the project having laid a solid foundation for future analyses and projects. While not "ideal" from a data analysis perspective, the particularities of both the Viganello and Trevano systems represent the reality where PV systems are installed. In theory, row-to-row distances should be identical, shading from surrounding buildings should be avoided, and usually only one technology is deployed on site. Instead, having seven technologies subject to row-to-row and building-to-string shading, more interesting results can be obtained as to the resilience and reliability of these technologies.

The RACONT2050 project itself is intended to last to 2050 with monitoring and data of the systems available until that point. It is fitting that this successor to the TISO-10 project is also continuing data capture of the TISO-10 modules, now over 43 years in operation.

Aspects that will be investigated in future will be:

- **Evaluating and understanding long-term system performance** through within-technology and within-company comparisons, with particular focus on the distinction between early stabilization vs. long-term degradation).
- **Root-cause analysis of first observed module failures** (e.g. potential shading induced glass breakage, interconnection failures).
- **Investigation of the impact of system voltage on long-term module reliability**, particularly for high-voltage (1500 Vdc) string configurations.
- **Determination of Performance Loss Rate (PLR)** determination and PR(tc) stability over time, and comparison with lab-based degradation measurements.
- **Comparing soiling sensor data to soiling determination in the field and in the lab** (measure P_{STC} before cleaning and after cleaning) and evaluate the usefulness of smaller soiling sensors (0.4 m to 1.1 m) compared to long (>2 m) PV modules.
- **Automated detection methods for glass breakage**, using monitoring data and diagnostic tools.
- **Definition of representative shading scenarios** occurring in commercial roof top systems for Shady-PV (BFE project).
- **Investigation of the occurrence and long-term evolution of hotspots on modules**, including the role of soiling, shading and module design.

Some of these activities will be also part of a follow-up project **SOLID-PV (Metrology supporting large-scale deployment of efficient and resilient photovoltaic systems, EURAMET 24GRD04),** started in June 2025.The new project, aims to reduce uncertainties in PV performance metrics by developing standards, calibration methods and models for accurate irradiance and performance measurements. It will harmonise uncertainty propagation, degradation assessment and monitoring practices, supported by reference PV systems and digital twins, enabling improved standards and sensor optimisation.

Within this framework, the follow-up activities are:

- The Viganello site will be deal as **reference system** and be upgraded with additional sensors, more in-field and in-lab measurements, and the monitoring data will be used to test and **validate PLR methodologies applicable to shaded systems**.
- An **open-source digital twin** of the system will be developed to support future research on performance prediction, degradation modelling and predictive maintenance.

- The complementary **benefits of field diagnostic tools** as dark I-V versus daylight I-V, as well as other measurement techniques (e.g. PLR from monitoring data, as well as EL, UVf or multi-spectral analysis developed within the project EAGLE) will be explored.
- The outcomes of this project will be used to support and improve the IEC 61724 (PV monitoring) standard and give **recommendations for the monitoring of commercial rooftop systems**.

6 Dissemination

[1] Samuele Chiesa, Gian Carlo Dozio, Domenico Chianese "Long-term monitoring of degradation and defect in high-voltage strings through dark I-V measurements", 41st EU PVSEC, Vienna, 2023.

[2] Domenico Chianese, Mauro Caccivio, Gabi Friesen, "RACONT2050: Reliability And Comparison of New PV Technologies", 41st EU PVSEC, Vienna, 2023.

Upcoming dissemination

[3] Bert Herteleer, Silvana Ovaitt, "What do PV Module Warranties Reveal about Reliability? Insights from Financial Disclosures and Independent Testing", 43rd EU PVSEC, September 2026, Rotterdam.

[4] Bert Herteleer, Ebrar Özkalay, Gabi Friesen, "Degradation is not PLR", 43rd EU PVSEC, September 2026, Rotterdam.

7 Awards

November 2024, Samuele Chiesa received the First Prize (CHF 3,000) from the Nizzola Foundation for his *Master of Science in Engineering* thesis at the Department of Innovative Technologies (DTI) of SUPSI on the innovative dark I-V measurement device for continuous monitoring of photovoltaic systems.

References

[1] B. Herteleer *et al.*, 'A Commodity Today, Incompatible Tomorrow: The Paradox of PV?', *42nd Eur. Photovolt. Sol. Energy Conf. Exhib.*, pp. 020574-001-020574–008, 2025, doi: 10.4229/EUPVSEC2025/5EP.1.3.

[2] C. Sen *et al.*, 'Buyer aware: Three new failure modes in TOPCon modules absent from PERC technology', *Sol. Energy Mater. Sol. Cells*, vol. 272, p. 112877, Aug. 2024, doi: 10.1016/j.solmat.2024.112877.

[3] M. U. Khan *et al.*, 'UV-induced degradation in TOPCon solar cells: Hydrogen dynamics and impact of UV wavelength', *Sol. Energy Mater. Sol. Cells*, vol. 294, p. 113895, Jan. 2026, doi: 10.1016/j.solmat.2025.113895.

[4] A. Realini, 'Mean Time Before Failure of Photovoltaic modules'.

[5] SUPSI ISAAC, *Photovoltaics: made to last. The 40 years of the TISO PV plant*. 2022. [Online]. Available: https://pvlab.solar/wp-content/uploads/2022/10/TISO_Catalogo_Web.pdf

[6] Alessandro Virtuani, Eleonora Annigoni, Christophe Ballif, Mauro Caccivio, Gabi Friesen, Domenico Chianese, Tony Sample, 'The 35th Birthday of the Tiso-10-kW Solar Plant: Lessons Learned in Safety and Performance', in *35th EU PVSEC 2018*, WIP. Accessed: Mar. 05, 2026. [Online]. Available: https://userarea.eupvsec.org/proceedings/35th-EU-PVSEC-2018/5DO.9.1/

[7] T. Friesen *et al.*, 'TISO 10 kW: 30 Years Experience with a PV Plant', *27th Eur. Photovolt. Sol. Energy Conf. Exhib. 3125-3131*, p. 7 pages, 6878 kb, 2012, doi: 10.4229/27THEUPVSEC2012-4DO.5.2.

[8] A. Virtuani *et al.*, '35 years of photovoltaics: Analysis of the TISO-10-kW solar plant, lessons learnt in safety and performance—Part 1', *Prog. Photovolt. Res. Appl.*, vol. 27, no. 4, pp. 328–339, 2019, doi: 10.1002/pip.3104.

[9] E. Annigoni, A. Virtuani, M. Caccivio, G. Friesen, D. Chianese, and C. Ballif, '35 years of photovoltaics: Analysis of the TISO-10-kW solar plant, lessons learnt in safety and performance—Part 2', *Prog. Photovolt. Res. Appl.*, vol. 27, no. 9, pp. 760–778, 2019, doi: 10.1002/pip.3146.

[10] K. Chen, J. Zuo, and R. Chang, 'Compendium of degradation rates of global photovoltaic (PV) technology: insights from technology, climate and geography', *Sol. Energy Mater. Sol. Cells*, vol. 293, p. 113839, Dec. 2025, doi: 10.1016/j.solmat.2025.113839.

[11] I. Kaaya and K.-A. Weiss, 'Physical and Data-driven Hybrid Model for Outdoor Lifetime Prediction of PV Modules', in *2020 47th IEEE Photovoltaic Specialists Conference (PVSC)*, Jun. 2020, pp. 0460–0464. doi: 10.1109/PVSC45281.2020.9300526.

[12] F. ibne Mahmood and G. TamizhMani, 'Impact of different backsheets and encapsulant types on potential induced degradation (PID) of silicon PV modules', *Sol. Energy*, vol. 252, pp. 20–28, Mar. 2023, doi: 10.1016/j.solener.2023.01.047.

[13] P. Hacke, S. Spataru, B. Habersberger, and Y. Chen, 'Field-representative evaluation of PID-polarization in TOPCon PV modules by accelerated stress testing', *Prog. Photovolt. Res. Appl.*, vol. 32, no. 5, pp. 346–355, 2024, doi: 10.1002/pip.3774.

[14] Associazione delle aziende elettriche svizzere AES, 'Prescrizzioni delle Aziende Elettriche CH (PAE-CH 2021)'. [Online]. Available: https://www.elettricita.ch/wp-content/uploads/2021/12/20211201-rs-prescrizioni-aziende-elettriche-ch-1.pdf

[15] Herrmann, W., Eder, G., Farnung, B., Friesen, G., Köntges, M., Kubicek, B., Kunz, O., Liu, H., Parlevliet, D., Tsanakas, I. and Vedde, J., 'Qualification of Photovoltaic (PV) Power Plants using Mobile Test Equipment', IEA PVPS Task 13, Report IEA-PVPS T13-24:2021, Apr. 2021.

[Online]. Available: https://iea-pvps.org/wp-content/uploads/2021/04/IEA-PVPS-T13-24_2021_Qualification-of-PV-Power-Plants_report.pdf

[16] 'IEC 61724-1:2021'. Accessed: Mar. 06, 2026. [Online]. Available: https://webstore.iec.ch/en/publication/65561

[17] M. Köntges, J. Lin, A. Virtuani, G. C. Eder, J. Zhu, G. Oreski, P. Hacke, J. S. Stein, L. Bruckman, P. Gebhardt, D. Barrit, M. Rasmussen, I. Martin, K. O. Davis, G. Cattaneo, B. Hoex, Z. Hameiri, E. Özkalay, 'Degradation and Failure Modes in New Photovoltaic Cell and Module Technologies', Report IEA-PVPS T13-30:2025, Feb. 2025. doi: 10.69766/ATBD2730.

[18] H. Lee, S. Cho, K. Yoon, and J. Lee, 'Glass Thickness and Fragmentation Behavior in Stressed Glasses', *New J. Glass Ceram.*, vol. 2, no. 4, pp. 116–121, Oct. 2012, doi: 10.4236/njgc.2012.24020.

[19] M. Braga *et al.*, 'Solar Over-Irradiance Events: Preliminary Results from a Global Study', in *2020 47th IEEE Photovoltaic Specialists Conference (PVSC)*, Jun. 2020, pp. 2764–2770. doi: 10.1109/PVSC45281.2020.9300868.

[20] Sascha Lindig, Julien Deck, Magnus Herz, Julián Ascencio Vásquez, Marios Theristis, Bert Herteleer, Kevin Anderson, 'Technical Key Performance Indicators for Photovoltaic Systems: Challenges and Best Practices', Report IEA-PVPS T13-28:2024, Dec. 2024. doi: https://doi.org/10.69766/LUZI3108.

[21] S. Lindig, J. Ascencio-Vásquez, J. Leloux, D. Moser, and A. Reinders, 'Performance Analysis and Degradation of a Large Fleet of PV Systems', *IEEE J. Photovolt.*, vol. 11, no. 5, pp. 1312–1318, Sep. 2021, doi: 10.1109/JPHOTOV.2021.3093049.

[22] G. Badran and M. Dhimish, 'A comparative study of bifacial versus monofacial PV systems at the UK's largest solar plant', *Clean Energy*, vol. 8, no. 4, pp. 248–260, Aug. 2024, doi: 10.1093/ce/zkae043.

[23] G. M. Tina, A. Osama, G. Mannino, A. Gagliano, A. V. Cucuzza, and F. Bizzarri, 'Thermal comparison of floating bifacial and monofacial photovoltaic modules considering two laying configurations', *Appl. Energy*, vol. 389, p. 125732, Jul. 2025, doi: 10.1016/j.apenergy.2025.125732.

[24] Joshua S Stein, Christian Reise, Johanna Bonilla Castro, Gabi Friesen, Giosuè Maugeri, Elías Urrejola, Samuli Ranta, 'Bifacial Photovoltaic Modules and Systems: Experience and Results from International Research and Pilot Applications', IEA PVPS, Report IEA-PVPS T13-14:2021, Apr. 2021. Accessed: Mar. 12, 2026. [Online]. Available: https://iea-pvps.org/key-topics/bifacial-photovoltaic-modules-and-systems/

[25] R. O. Yakubu, L. D. Mensah, D. A. Quansah, and M. S. Adaramola, 'A systematic literature review of the bifacial photovoltaic module and its applications', *J. Eng.*, vol. 2024, no. 8, p. e12421, 2024, doi: 10.1049/tje2.12421.

Annex

Average degradation in Pm, Isc, Voc and FF measured for replaced and reference modules together with the manufacturer warranty declarations.
For the reference modules Pm degradation of single modules is given in dependence of position in the string.

MODULE TYPES		WARRANTY		DEGRADATION 10 months* REPLACED MODULES (01.12.2022-27.09.2023)				DEGRADATION 13 months RFERENCE MODULES (29.09.2023-22.10.2024)							
Brand	**cell technology**	1st year degrad.	Annual degrad.	**avg. Pm**	avg. Voc	avg. Isc	avg. FF	**avg. Pm**	*Pm REF1 (pos)*	*Pm REF2 (neg)*	*Pm REF3 (centre)*	*Pm REF4 (centre)*	avg. Voc	avg. Isc	avg. FF
A	PERC mono-facial half-cut	-1%	-0.4 %	-0.71%	-0.35%	-0.04%	-0.31%	-1.11%	*-1.71%*	*-1.87%*	*-1.82%*	*-2.49%*	-0.23%	-0.46%	-0.42%
B	PERC bifacial shingled	-2%	-0.45 %	-0.94%	-0.71%	-0.36%	0.13%	-1.53%	*-4.93%*	*-5.16%*	*-5.10%*	*-5.21%*	-0.79%	-0.56%	-0.19%
C1	TOPCon n-type mono-facial half-	-1%	-0.4 %	-0.36%	-0.23%	0.00%	-0.13%	-0.59%	*-2.28%*	*-2.36%*	*-2.37%*	*-2.43%*	-0.41%	-0.28%	0.09%
C2	TOPCon n-type bifacial half-cut	-1%	-0.4 %	-0.64%	-0.34%	-0.27%	-0.03%	-0.93%	*-3.00%*	*-3.25%*	*-3.20%*	*-3.00%*	-0.41%	-0.61%	0.09%
D	HJT bifacial half-cut	-1%	-0.2 %	-2.22%	-0.72%	-1.06%	-0.46%	-4.07%	*-6.11%*	*-7.41%*	*-5.70%*	*-6.31%*	-1.20%	-1.98%	-0.95%
E1	PERC mono-facial half-cut	-2%	-0.55 %	-1.52%	-1.22%	-0.15%	-0.15%	-1.62%	*-1.58%*	*-2.01%*	*-2.08%*	*-1.97%*	-1.27%	0.00%	-0.35%
E2	TOPCon n-type bifacial half-cut	-1%	-0.4 %	-0.30%	-0.36%	0.54%	-0.47%	-0.67%	*-2.77%*	*-2.74%*	*-2.79%*	*-3.17%*	-0.55%	0.10%	-0.22%

Examples of electroluminescence images measured before and after field exposure for all 7 technologies.

	Tech #1 - PERC	Tech #2 –PERC/shingl	Tech #3 - TOPCon	Tech #4 - TOPCon	Tech #5 - HJT	Tech #6 - PERC	Tech #7 - TOPCon
out of teh box	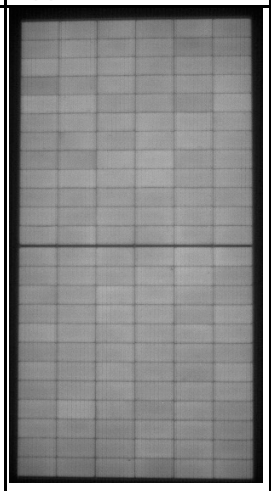	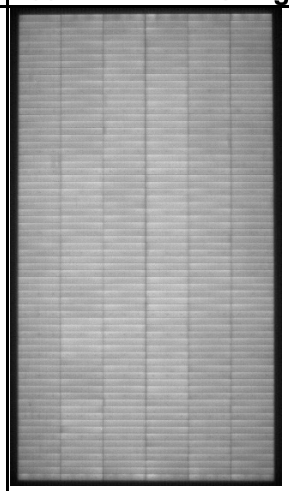	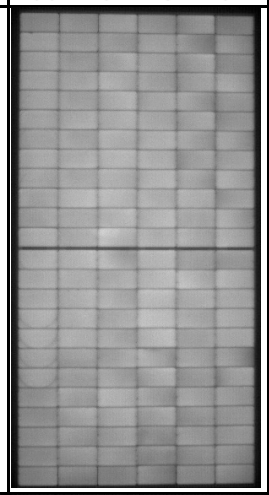	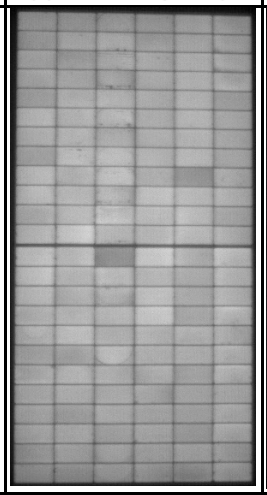	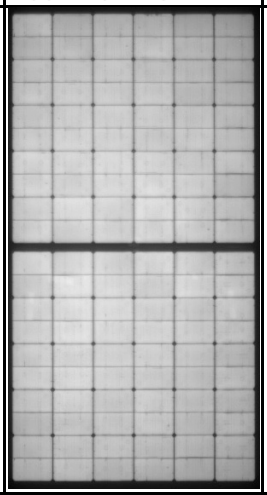	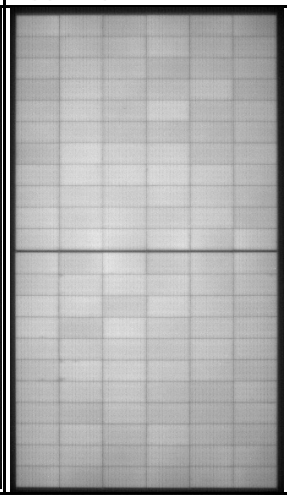	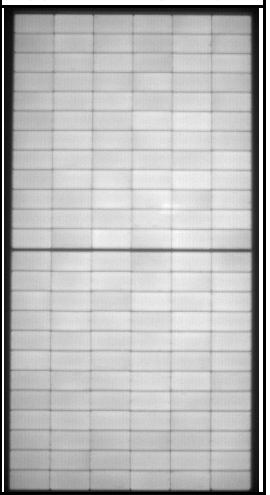
after 13 months of field exposure